ARTICLE IN PRESS

Ecological Indicators xxx (xxxx) xxx–xxx

Contents lists available at ScienceDirect

Ecological Indicators

journal homepage: www.elsevier.com/locate/ecolind

Original Articles

Indicators for contaminant transport in a three-layer wetland with wind

Huilin Wang[a], Bin Chen[b], Ping Wang[c], Wenxin Huai[a,*], Jing Luo[a]

[a] State Key Laboratory of Water Resources and Hydropower Engineering Science, Wuhan University, Wuhan 430072, China
[b] State Key Laboratory of Water Environment Simulation, School of Environment, Beijing Normal University, Beijing 100875, China
[c] Key Laboratory of State Forestry Administration on Soil and Water Conservation, School of Soil and Water Conservation, Beijing Forestry University, Beijing 100083, China

ARTICLE INFO

Keywords:
Three-layer wetland
Dispersion
Ecological degradation
Wind effect

ABSTRACT

The effect of global climate change is increasing and it can influence agriculture in many ways, especially in that it makes great threaten on agricultural water resources. Since agricultural water supply is a key issue for agricultural production, indicators for contaminant transport in wetlands should be considered in order to solve agricultural water pollution and promote water protection. In this paper, we analyze the environmental dispersion in a typical three-layer wetland flows with the effect of wind taken into account. The analytical solution for velocity distribution is rigorously derived and the dependence of characteristic parameters on averaged dimensionless velocity is recorded. The asymptotic analysis theory of Gill is employed to measure dispersivity for natural wetland flows with a commonly high *Peclet* number. Both velocity and environmental dispersion are significantly influenced by wind, in terms of its direction and the magnitude of force. The effects of hydraulics and ecological degradation are considered to obtain the analytical solution for the mean concentration and maximal critical length of the region influenced by the process of contaminant transport.

1. Introduction

As an essential element of ecological systems, wetlands serve a series of fundamental functions, such as ecological restoration, water supply, water purification, greenhouse effect mitigation, climate regulation and biodiversity preservation (Costanza et al., 1989, 1997). The effective management of water and fertilizer in agriculture is challenged by the global climate change, which consequently changes the drainage of agriculture and significantly affects wetlands (Mitsch and Hernandez, 2013). As an effective way to cope with the agricultural non-point source pollution, which has become increasingly prominent in recent decades, agricultural riparian wetlands play a key role in contaminant degradation and retardation (Kao and Wu, 2001; Wang and Chen, 2016). Conversely, it has been revealed as well that effluent of domestic wastewater treated by wetlands will be suitable for reuse in agriculture (Lavrnic and Mancini, 2016). Contaminants transport process in wetland flow has emerged as a significant issue in environmental risk assessment and wastewater treatment engineering in natural and constructed wetlands (Carvalho et al., 2009; Costanza et al., 1997; US EPA, 1999). However, the mechanisms underlying these transport processes have yet to be investigated thoroughly, and the most important work is to predict the critical length and duration of the region which forms an instantaneous contaminant release (Chen et al., 2010; Zeng and Chen, 2011).

The asymptotic contaminant transport process in wetland flows is termed as environmental dispersion, which can be explored at the environmental macroscopic scale by treating the wetland as a porous medium. In this scale, the contaminant clouds spread toward the longitudinal direction under the combined effects of vertical concentration dispersion and apparent vertical velocity non-uniformity (Zeng and Chen, 2009). Considering specific characteristic of wetlands, Chen et al. (2010), Zeng et al. (2011), Zeng et al. (2012), and Wu et al. (2011b) investigated contaminant transport processes in wetland flows at a phase-averaged scale, which is the start point for the recent analyses of contaminant dispersion in wetland flows.

Based on the Taylor's theory (1953), the dispersivity in wetland flows has been studied through different approaches. Zeng et al. (2012) investigated the effect of wind on environmental dispersion in a single-layer wetland through the concentration moments method, which was first introduced by Aris (1956). Wu et al. (2011a) further applied this method to examine the solute dispersion in a two-zone wetland. Through the classical multi-scale method that first proposed by Mei et al. (1996), Chen and Wu (2012) suggested that two time scales are sufficient for the analysis of the long-time evolution of solute clouds. Then multi-scale method has been extended (Wu and Chen, 2014a; Wu and Chen, 2014b; Zeng et al., 2015) to address the transverse

* Corresponding author.
E-mail address: wxhuai@whu.edu.cn (W. Huai).

https://doi.org/10.1016/j.ecolind.2018.04.005
Received 26 May 2017; Received in revised form 29 January 2018; Accepted 3 April 2018
1470-160X/

Please cite this article as: Wang, H., Ecological Indicators (2018), https://doi.org/10.1016/j.ecolind.2018.04.005

concentration distribution, and the simple and elegant pattern of the spatial distribution formed during the Taylor dispersion process has also been characterized (Wu et al. 2016). Wang et al. (2015) employed multi-scale analysis to determine the concentration dispersion in a three-zone wetland. Asymptotic analysis based on Gill's theory (1967) has also been applied (Wu and Chen, 2012; Chen, 2013; Wang et al., 2013; Luo et al., 2016). By an asymptotic method the steady status of dispersion can be evaluated and complications in asymptotic variation can be prevented.

Wetlands are complex ecological-hydraulic systems, and their heterogeneity is generally attributed to the inhomogeneous distribution of vegetation and substrate material. Considering the effect of the heterogeneity of medium distribution, researchers have analyzed environmental dispersivity in different types of wetlands. For instance, Murphy et al. (2007) used a two-zone model to evaluate the relationship between relative submergence and longitudinal dispersivity in channels. Wu et al. (2011a) assessed the dispersion of flow in a two-zone wetland and provided an analytical solution to predict dispersivity in the two-zone type of width-dominated wetlands. Wang et al. (2015) investigated environmental dispersion in a three-zone wetland through multi-scale analysis. Luo et al. (2016) also explored three-zone wetlands through asymptotic analysis. While for the depth-dominated deep wetlands, Chen et al. (2012) examined the dispersivity in a two-layer wetland flow, and Wang et al. (2013) evaluated the solute dispersion in a three-layer wetland flow dominated by a free surface. Since the single- and two-layer wetlands can be regarded as special cases of three-layer wetlands (Wang et al., 2013), the wetlands studied in this paper can also turn into two- or single-layer wetlands under certain conditions.

However, the effect of wind, which contributes to environmental dispersion, has been rarely analyzed. Blowing over the free surface of the wetlands, wind can exert a drag at the air-water interface, and consequently affect the sediment dispersion process dramatically (Sheng and Lick, 1979). Thus, wind can considerably affect the velocity profile in natural wetland flows as wind force changes (Zeng et al., 2012). Wind can even form an inverse flow layer when it moves in the opposite direction of flows. Consequently, environmental dispersion can be influenced indirectly (Wu, 1969). Therefore, the effect of wind should be considered during the analysis of the velocity profile and dispersivity in realistic wetlands. Zeng et al. (2012) primarily investigated the influence of wind on environmental dispersion in single-layer wetland flows on the basis of concentration moments method. However, as they disregarded inhomogeneity, studies have also yet to analyze the effects of wind on three-layer wetlands which are typical in nature, such as stems or pleuston in the top layer, submerged vegetation in the interlayer, and roots or gravels in the bottom layer.

Ecological effects, such as absorption, bacterial metabolism, and hydrolysis, are important factors that influence dispersivity in wetland flows. A simplified asymptotic approach must be applied to provide an analytical solution on dispersivity by considering ecological degradation as a relevant factor to incorporate additional elements affecting contaminant transport processes in wetlands. Although Wu et al. (2015) discussed the vertical distribution of contaminants based on asymptotic variation, the status of this parameter would become increasingly complex when wind is considered.

This study examines environmental dispersion in a three-layer wetland flow affected not only by hydraulics but also by wind and ecological factors. As an extension of the research on the effect of wind on dispersivity in single-layer wetlands, this paper aims to (a) illustrate the velocity profile of the three-layer wetland flow affected by wind; (b) determine solute dispersion by applying a simplified approach; (c) obtain an analytical solution for environmental dispersivity by considering ecological and hydraulic effects; and (d) give an application for predicting duration and maximum length of the contaminant influenced region.

2. Formulation for momentum and concentration transport

The following equations for the momentum and concentration transport in a typical wetland flow can be adopted at the phase scale (Liu and Masliyah, 2005; Zeng and Chen, 2009; Zeng et al., 2011):

$$\rho\left(\frac{\partial \mathbf{U}}{\partial t} + \nabla\cdot\frac{\mathbf{U}\mathbf{U}}{\phi}\right) = -\nabla P - \mu F\mathbf{U} + \kappa\mu\nabla^2\mathbf{U} + \kappa\nabla\cdot(\mathbf{L}\cdot\nabla\mathbf{U}) \tag{1}$$

and

$$\phi\frac{\partial C}{\partial t} + \nabla\cdot(\mathbf{U}C) = \nabla\cdot(\kappa\lambda\phi\nabla C) + \kappa\nabla\cdot(\mathbf{K}\cdot\nabla C) \tag{2}$$

where ρ denotes density (kg m^{-1}), $\mathbf{U}$ denotes velocity (ms^{-1}), t denotes time (s), ϕ denotes porosity (dimensionless), P denotes pressure (kg m^{-1} s^{-2}), μ denotes dynamic viscosity (kg m^{-1} s^{-1}), F denotes shear factor (m^{-2}), κ denotes tortuosity (dimensionless) to treat the spatial structure of porous media, $\mathbf{L}$ denotes the momentum dispersivity tensor (kg m^{-1} s^{-1}), C denotes concentration (kg m^{-3}), λ denotes mass diffusivity (m^2 s^{-1}), and $\mathbf{K}$ denotes mass dispersivity tensor (m^2 s^{-1}). To smooth the discontinuity between the two phases of water and plants, concentration dispersivity can be analyzed at the phase-averaged scale. Given the flow characteristics in three-layer wetlands, the Eq. (1) for momentum transport is based on the Navier–Stokes equation

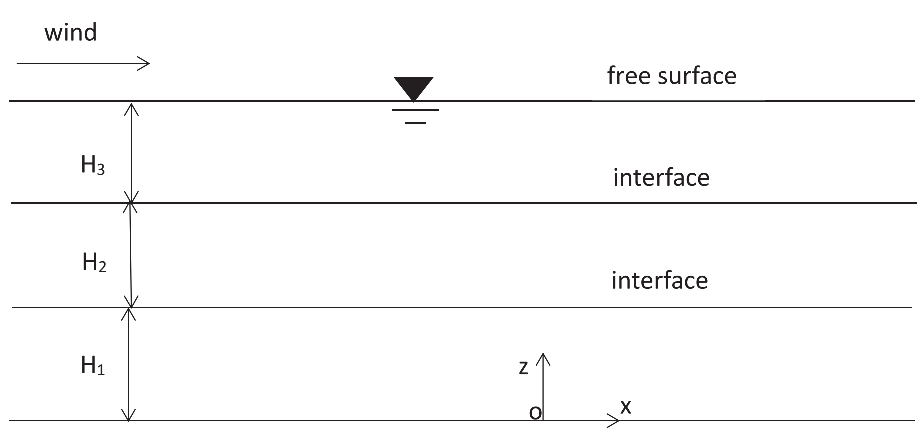

Fig. 1. Sketch of a three-layer wetland flow under the influence of wind.

for single phase flows and Darcy's law for the sweeping flow in porous media. The Eq. (2) for concentration transport is derived analogously from a combination of the concentration dispersion law and the advective–diffusive equation.

The solute moves in a fully developed unidirectional steady flow in a three-layer wetland with a depth of H ($H = H_1 + H_2 + H_3$) as illustrated in Fig. 1. H_1, H_2, and H_3 represent the height of layers 1, 2, and 3, respectively, with each layer assuming the constant ϕ, F, κ, $\mathbf{L}$, and $\mathbf{K}$. The flow direction aligns with the longitudinal x-axis, the z-axis represents the vertical direction and the origin is set at the bottom in a right-handed Cartesian coordinate system. And the effect of wind is considered in this illustration.

By appending the effect of wind parallel to the flow direction, Eq. (1) can be reduced for the three-layer unidirectional flow as follows:

$$\kappa_1(\mu + L_1)\frac{d^2u_1}{dz_1^2} - \mu F_1 u_1 - \frac{dp}{dx} = 0, 0 \leqslant z_1 \leqslant H_1 \tag{3}$$

$$\kappa_2(\mu + L_2)\frac{d^2u_2}{dz_2^2} - \mu F_2 u_2 - \frac{dp}{dx} = 0, H_1 \leqslant z_2 \leqslant H_1 + H_2 \tag{4}$$

and

$$\kappa_3(\mu + L_3)\frac{d^2u_3}{dz_3^2} - \mu F_3 u_3 - \frac{dp}{dx} = 0, H_1 + H_2 \leqslant z_3 \leqslant H_1 + H_2 + H_3 \tag{5}$$

where u_1, u_2, and u_3 denote longitudinal velocities, κ_1, κ_2, and κ_3 denote the tortuosities, L_1, L_2, and L_3 denote the momentum dispersivities, and F_1, F_2, and F_3 denote the shear factors in layers 1, 2, and 3, respectively.

The non-slip condition at the bed of $z_1 = 0$ and the wind stress condition with the free surface of $z_3 = H$ can be expressed as follows:

$$u_1(z_1)|_{z_1=0} = 0, \kappa_3(\mu + L_3)\frac{du_3}{dz_3}\bigg|_{z_3=H} = \frac{1}{2}\omega C_d \rho_{air} U_{wind}^2 \tag{6}$$

where ω denotes the direction of wind that affects the wetland flow, C_d is the drag coefficient of wind, ρ_{air} is the air density, and U_{wind} is the wind velocity. The wind enhances the wetland flow when $\omega = 1$, but weakens the wetland flow when $\omega = -1$.

The following equations represent the continuity of velocity and stress at the interfaces of the two adjacent layers:

$$u_1(z_1)|_{z_1=H_1} = u_2(z_2)|_{z_2=H_1} \tag{7}$$

$$u_2(z_2)|_{z_2=H_1+H_2} = u_3(z_3)|_{z_3=H_1+H_2} \tag{8}$$

$$\kappa_1(\mu + L_1)\frac{du_1}{dz_1}\bigg|_{z_1=H_1} = \kappa_2(\mu + L_2)\frac{du_2}{dz_2}\bigg|_{z_2=H_1}, \tag{9}$$

and

$$\kappa_2(\mu + L_2)\frac{du_2}{dz_2}\bigg|_{z_2=H_1+H_2} = \kappa_3(\mu + L_3)\frac{du_3}{dz_3}\bigg|_{z_3=H_1+H_2} \tag{10}$$

Under a uniform and instantaneous contaminant release with mass Q (kg m^{-1}) at the cross section of $x = 0$ at time $t = 0$, the initial contaminant concentration can be expressed as follows:

$$C_k(x,z_k,t)|_{t=0} = \frac{Q\delta(x)}{\phi_k H}, k = 1,2,3 \tag{11}$$

where $\delta(x)$ is the Dirac delta function, C_k is the contaminant concentration, and ϕ_k denotes the porosities for layers 1, 2, and 3.

If the released contaminant has a finite amount, then the boundary condition for the contaminant concentration can be expressed as follows:

$$C_k(x,z_k,t)|_{x=\pm\infty} = 0, k = 1,2,3 \tag{12}$$

Following Wu et al. (2011a,b), by regarding the contaminant transport process in a fully developed unidirectional flow through a three-layer wetland, Eq. (2) can be reduced as follows:

$$\frac{\partial C_k}{\partial t} + \frac{u_k}{\phi_k}\frac{\partial C_k}{\partial x} = \kappa_k\left(\lambda_k + \frac{K_{xk}}{\phi_k}\right)\frac{\partial^2 C_k}{\partial x^2} + \kappa_k\left(\lambda_k + \frac{K_{zk}}{\phi_k}\right)\frac{\partial^2 C_k}{\partial z_k^2}, k = 1,2,3 \tag{13a}$$

The effect of longitudinal dispersion can be neglected since natural wetlands have a high *Peclet* number commonly (Chen et al., 2012). Therefore, the above equation can be simplified as follows:

$$\frac{\partial C_k}{\partial t} + \frac{u_k}{\phi_k}\frac{\partial C_k}{\partial x} = \kappa_k\left(\lambda_k + \frac{K_{zk}}{\phi_k}\right)\frac{\partial^2 C_k}{\partial z_k^2}, k = 1,2,3, \tag{13b}$$

where λ_k denotes the concentration diffusivities, K_{xk} denotes the longitudinal concentration dispersivities, and K_{zk} denotes the vertical concentration dispersivities for layers 1, 2, and 3.

Considering the bed at the bottom $z_1 = 0$ and the free surface at $z_3 = H$, the non-penetrative conditions can be expressed as follows:

$$\frac{\partial C_1(x,z_1,t)}{\partial z_1}\bigg|_{z_1=0} = \frac{\partial C_3(x,z_3,t)}{\partial z_3}\bigg|_{z_3=H} \tag{14}$$

The continuity of the concentration and flux at the interfaces of adjacent layers can be expressedas follows:

$$C_1(x,z_1,t)|_{z_1=H_1} = C_2(x,z_2,t)|_{z_2=H_1} \tag{15}$$

$$C_2(x,z_2,t)|_{z_2=H_1+H_2} = C_3(x,z_3,t)|_{z_3=H_1+H_2} \tag{16}$$

$$\kappa_1\left(\lambda_1 + \frac{K_{z1}}{\phi_1}\right)\frac{\partial C_1}{\partial z_1}\bigg|_{z_1=H_1} = \kappa_2\left(\lambda_2 + \frac{K_{z2}}{\phi_2}\right)\frac{\partial C_2}{\partial z_2}\bigg|_{z_2=H_1} \tag{17}$$

and

$$\kappa_2\left(\lambda_2 + \frac{K_{z2}}{\phi_2}\right)\frac{\partial C_2}{\partial z_2}\bigg|_{z_2=H_1+H_2} = \kappa_3\left(\lambda_3 + \frac{K_{z3}}{\phi_3}\right)\frac{\partial C_3}{\partial z_3}\bigg|_{z_2=H_1+H_2} \tag{18}$$

3. Analysis of environmental dispersion

3.1. Velocity profile

The following dimensionless parameters are used:

$$\eta_k = \frac{z_k}{H} \tag{19}$$

and

$$\psi_k = \frac{u_k}{u_c} \tag{20}$$

where

$$u_c = -\frac{dp}{dx}\frac{H^2}{[\kappa_1(\mu + L_1)\kappa_2(\mu + L_2)\kappa_3(\mu + L_3)]^{1/3}} \tag{21}$$

is the characteristic velocity of flow in a three-layer wetland.

Eqs. (3) to (10) can be non-dimensionalized as follows:

$$\frac{d^2\psi_1}{d\eta_1^2} - N_1 M_1 \alpha^2 \psi_1 + M_1 = 0, 0 \leqslant \eta_1 \leqslant r \tag{22}$$

$$\frac{d^2\psi_2}{d\eta_2^2} - N_2 M_2 \alpha^2 \psi_2 + M_2 = 0, r \leqslant \eta_2 \leqslant \theta \tag{23}$$

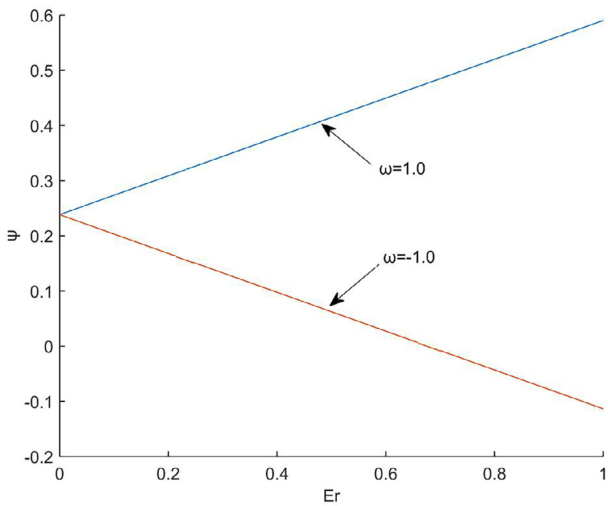

Fig. 2. Variation of $\overline{\psi}$ with $\boldsymbol{E_r}$.

$$\frac{d^2\psi_3}{d\eta_3^2} - N_3M_3\alpha^2\psi_3 + M_3 = 0, \theta \leqslant \eta_2 \leqslant 1 \tag{24}$$

$$\psi_1(\eta_1|_{\eta_1=0}) = 0, \left.\frac{d\psi_3}{d\eta_3}\right|_{\eta_3=1} = \omega E_r M_3 \tag{25}$$

$$\psi_1(\eta_1|_{\eta_1=r}) = \psi_2(\eta_2|_{\eta_2=r}) \tag{26}$$

$$\psi_2(\eta_2|_{\eta_2=\theta}) = \psi_3(\eta_3|_{\eta_3=\theta}) \tag{27}$$

$$M_1^{-1}\frac{d\psi_1}{d\eta_1}|_{\eta_1=r} = M_2^{-1}\left.\frac{d\psi_2}{d\eta_2}\right|_{\eta_2=r}, \tag{28}$$

and

$$M_2^{-1}\left.\frac{d\psi_2}{d\eta_2}\right|_{\eta_2=\theta} = M_3^{-1}\left.\frac{d\psi_3}{d\eta_3}\right|_{\eta_3=\theta} \tag{29}$$

where $\boldsymbol{r}$ is the relative depth of layer 1 and can be expressed as follows:

$$r = \frac{H_1}{H} \tag{30}$$

while θ is the relative depth of layer 2 and can be expressed as follows:

$$\theta = \frac{H_1 + H_2}{H} \tag{31}$$

The relative magnitudes of the effective viscosities and viscous frictions of the zones can be expressed as follows:

$$M_k = \frac{[\kappa_1(\mu + L_1)\kappa_2(\mu + L_2)\kappa_3(\mu + L_3)]^{1/3}}{\kappa_k(\mu + L_k)}, k = 1,2,3 \tag{32}$$

and

$$N_k = \frac{F_k}{(F_1F_2F_3)^{1/3}}, k = 1,2,3 \tag{33}$$

The dimensionless parameters $\boldsymbol{M}$ and $\boldsymbol{N}$ must satisfy the following conditions:

$$M_1{\cdot}M_2{\cdot}M_3 = 1 \tag{34}$$

$$N_1{\cdot}N_2{\cdot}N_3 = 1 \tag{35}$$

$$\boldsymbol{E_r} = -\frac{(C_d\rho_{air}U_{wind}^2)/(2H)}{dp/dx} \tag{36}$$

and

$$\alpha = \left[\frac{F_1F_2F_3\mu^3}{\kappa_1(\mu + L_1)\kappa_2(\mu + L_2)\kappa_3(\mu + L_3)}\right]^{1/6}{\cdot}H \tag{37}$$

where $\boldsymbol{E_r}$ reflects the relative strength of wind force and effective pressure gradient, and α is a characteristic parameter that represents the combined action of the depth of the channel, the viscous friction of vegetation, the viscosity of the water body, the microscopic curvature of the flow passage, and the vertical momentum dispersion.

Solving Eqs. (22) to (29) yields the following:

$$\psi_1(\eta_1) = \Omega_1{\cdot}e^{\alpha\sqrt{N_1M_1}\eta_1} + \Omega_2{\cdot}e^{-\alpha\sqrt{N_1M_1}\eta_1} + \frac{1}{\alpha^2N_1}, \tag{38}$$

$$\psi_2(\eta_2) = \Omega_3{\cdot}e^{\alpha\sqrt{N_2M_2}\eta_2} + \Omega_4{\cdot}e^{-\alpha\sqrt{N_2M_2}\eta_2} + \frac{1}{\alpha^2N_2} \tag{39}$$

and

$$\psi_3(\eta_3) = \Omega_5{\cdot}e^{\alpha\sqrt{N_3M_3}\eta_3} + \Omega_6{\cdot}e^{-\alpha\sqrt{N_3M_3}\eta_3} + \frac{1}{\alpha^2N_3} \tag{40}$$

,where the coefficients Ω_1–Ω_6 are presented in Appendix A.

The average operator f is defined as follows:

$$\overline{f} = \int_0^r f_1 d\eta_1 + \int_r^\theta f_2 d\eta_2 + \int_\theta^1 f_3 d\eta_3 \tag{41}$$

Therefore, the corresponding depth-averaged velocity is computed as follows:

$$\begin{aligned}\overline{\psi} = {} & \frac{1}{N_3\alpha^2} + \frac{\theta(N_3 - N_2)}{N_2N_3\alpha^2} + \frac{r(N_2 - N_1)}{N_1N_2\alpha^2} \\ & + \frac{1}{\alpha\sqrt{M_3N_3}}\left[\Omega_5(\sigma_1 - \sigma_4) + \Omega_6\left(\frac{1}{\sigma_1} - \frac{1}{\sigma_4}\right)\right] \\ & + \frac{1}{\alpha\sqrt{M_1N_1}}\left[\Omega_1(\sigma_3 - 1) - \Omega_2\left(\frac{1}{\sigma_3} - 1\right)\right] \\ & + \frac{1}{\alpha\sqrt{M_2N_2}}\left[\Omega_3(\sigma_5 - \sigma_2) - \Omega_4\left(\frac{1}{\sigma_5} - \frac{1}{\sigma_2}\right)\right],\end{aligned} \tag{42}$$

$$\sigma_1 = e^{\alpha\sqrt{M_3N_3}} \tag{43}$$

$$\sigma_2 = e^{\alpha r\sqrt{M_2N_2}} \tag{44}$$

$$\sigma_3 = e^{\alpha r\sqrt{M_1N_1}} \tag{45}$$

$$\sigma_4 = e^{\alpha\theta\sqrt{M_3N_3}} \tag{46}$$

$$\sigma_5 = e^{\alpha\theta\sqrt{M_2N_2}} \tag{47}$$

Fig. 2 shows the relationship between $\overline{\psi}$ and $\boldsymbol{E_r}$ for $\alpha = 1.0$, $M_k = 1.0$, $N_k = 1.0$, $r = 1/3$, $\theta = 2/3$, and $\omega = \pm 1.0$. In this case, the three-layer wetland is converted into a single-layer wetland, and the results are similar to those of Zeng et al. (2012). Thus, the validity of the results is verified. The mean velocity of flow in wetlands increases as $\boldsymbol{E_r}$ increases when $\omega = 1$, whereas the mean velocity of flow decreases as $\boldsymbol{E_r}$ decreases when $\omega = -1$. These results suggest that wind can either reinforce or recede conveyance when wind direction changes as reflected in the changing valence of ω. Therefore, ω is a principal element for changing the conveyance capacity of wetland flows.

Figs. 3–7 show the dependence between ψ and dimensionless characteristic parameters ($\boldsymbol{E_r}$, α, M, N, r, θ). The results in Fig. 3(a) and (b) are similar to those of Zeng et al. (2012). As shown in Fig. 3(b), the

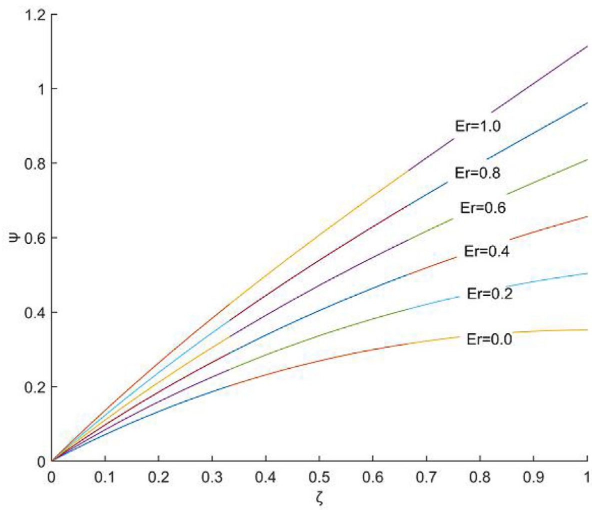

(a)

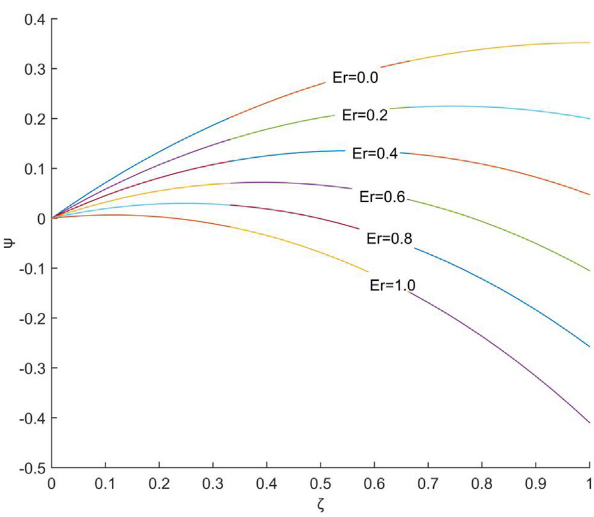

(b)

Fig. 3. Variation of non-dimensional velocity with depth (a) $\omega = 1$; (b) $\omega = -1$.

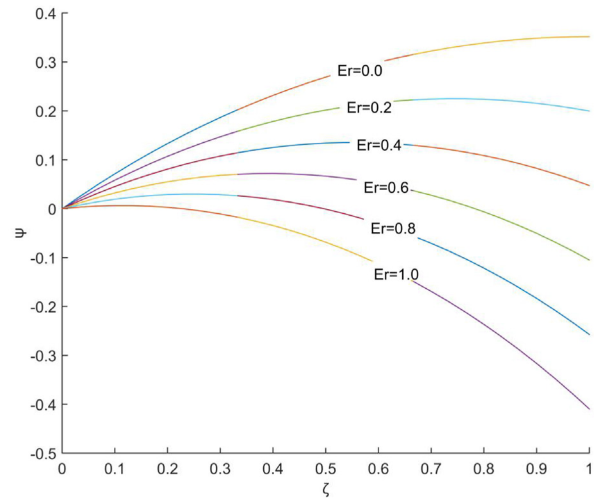

(a)

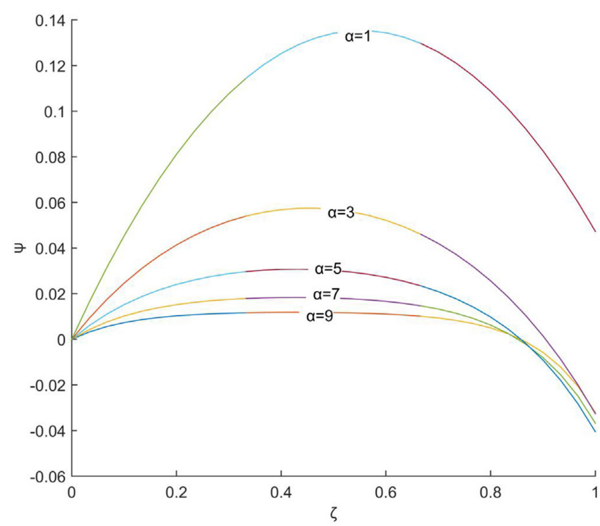

(b)

Fig. 4. Variation of ψ with ζ for $M_k = 1.0$, $N_k = 1.0$, $r = 1/3$, $\theta = 2/3$ and $\boldsymbol{E_r} = 0.4$: (a) $\omega = 1.0$ and (b) $\omega = -1$.

valence of $\overline{\psi}$ changes along with increasing $\boldsymbol{E_r}$, which indicates that an inverse flow layer may occur when the flow direction is against the wind.

3.2. Asymptotic analysis of environmental dispersion

The following dimensionless parameters are used:

$$\xi = \frac{x - \overline{u}_\phi t}{l_c}, \tau = \frac{t}{T_c}, \eta_k = \frac{z_k}{H}, k = 1,2,3 \tag{48}$$

where $\overline{u_\phi}$ is the average phase velocity based on the following:

$$u_{\phi k} = \frac{u_k}{\phi_k} \tag{49}$$

and

$$l_c = T_c \cdot u_c, \tag{50}$$

where l_c is a parameter that represents the characteristic length of the concentration cloud, and uc is the characteristic velocity of the flow as defined in Eq. (21).

Using the non-dimensional method yields the following:

$$\psi_{\phi k} = \frac{u_{\phi k}}{u_c}, k = 1,2,3 \tag{51}$$

.

$T_c \equiv \max\{T_1, T_2, T_3\}$ is associated with the following:

$$T_k = \frac{H^2}{\kappa_k(\lambda_k + (K_k/\phi_k))}, k = 1,2,3 \tag{52}$$

By applying the dimensionless method to the governing equations and boundary conditions, Eqs. (13b) to (18) can be rewritten as follows:

$$\frac{\partial C_k}{\partial \tau} + \psi'_{\phi k}\frac{\partial C_k}{\partial \xi} = \frac{T_c}{T_k}\frac{\partial^2 C_k}{\partial \eta_k^2}, k = 1,2,3 \tag{53}$$

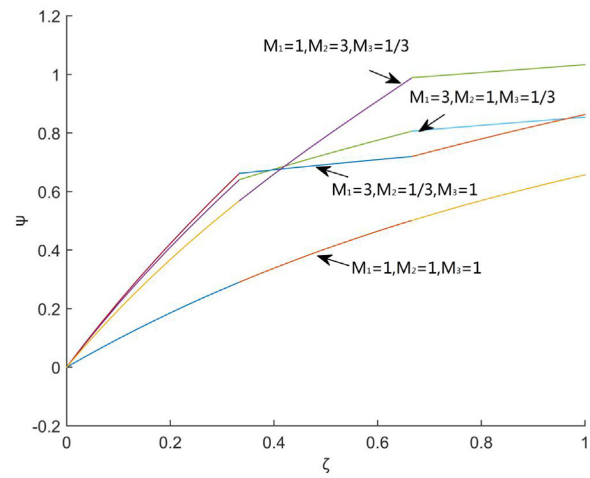

(a)

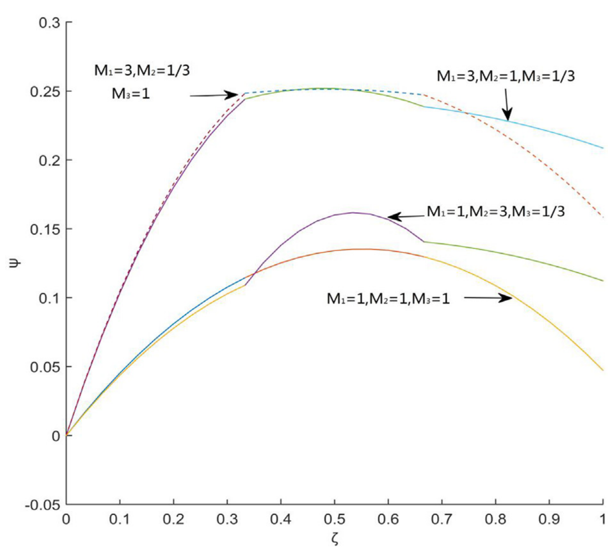

(b)

Fig. 5. Variation of ψ with ζ for $N_k = 1.0$, $\boldsymbol{E_r} = 0.4$, $r = 1/3$, $\theta = 2/3$ and $\alpha = 1.0$: (a) $\omega = 1.0$; (b) $\omega = -1.0$.

where

$$\psi'_{\phi k} = \psi_{\phi k} - \overline{\psi}_{\phi}, k = 1,2,3 \tag{54}$$

The dimensionless concentration deviations in layers 1, 2, and 3 are expressed as follows:

$$\left.\frac{\partial C_1}{\partial \eta_1}\right|_{\eta_1=0} = \left.\frac{\partial C_3}{\partial \eta_3}\right|_{\eta_3=1} = 0 \tag{55}$$

$$T_1^{-1}\left.\frac{\partial C_1}{\partial \eta_1}\right|_{\eta_1=r} = T_2^{-1}\left.\frac{\partial C_2}{\partial \eta_2}\right|_{\eta_2=r} \tag{56}$$

$$T_2^{-1}\left.\frac{\partial C_2}{\partial \eta_2}\right|_{\eta_2=\theta} = T_3^{-1}\left.\frac{\partial C_3}{\partial \eta_3}\right|_{\eta_3=\theta} \tag{57}$$

$$C_1|_{\eta_1=r} = C_2|_{\eta_2=r}, \tag{58}$$

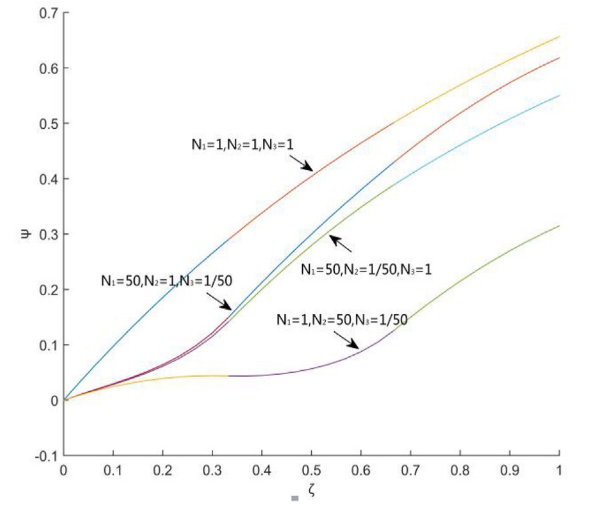

(a)

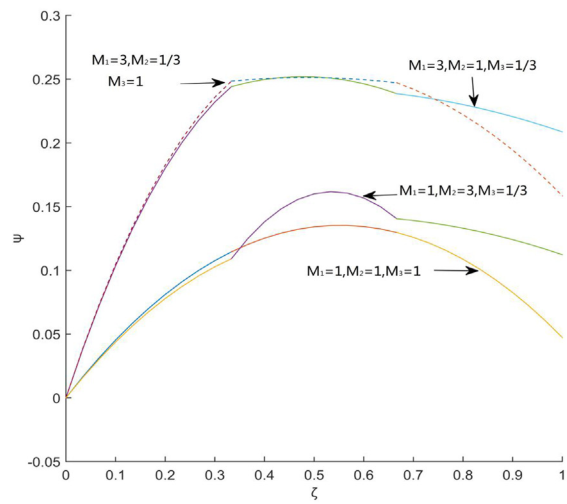

(b)

Fig. 6. Variation of ψ with ζ for $M_k = 1.0$, $\boldsymbol{E_r} = 0.4$, $r = 1/3$, $\theta = 2/3$, and $\alpha = 1.0$: (a) $\omega = 1.0$; (b) $\omega = -1.0$.

and

$$C_2|_{\eta_2=\theta} = C_3|_{\eta_3=\theta} \tag{59}$$

Averaging Eq. (53) with the method defined in Eq. (41) yields the following:

$$\frac{\partial \overline{C}}{\partial \tau} + \overline{\psi'_{\phi}\frac{\partial C'}{\partial \xi}} = 0 \tag{60}$$

By resolving C_k as $C_k = \overline{C} + C'_k$ and following the theory of Gill (1967) for dispersion in tube flows, the series expansions for concentration deviations are set as follows:

$$C'_k = G_k^{(1)}(\eta_k)\frac{\partial \overline{C}}{\partial \xi} + G_k^{(2)}(\eta_k)\frac{\partial^2 \overline{C}}{\partial \xi^2} + \cdots, k = 1,2,3 \tag{61}$$

Substituting Eq. (61) into Eq. (60) yields the following:

$$\frac{\partial \overline{C}}{\partial \tau} + \overline{\psi'_{\phi}\frac{\partial}{\partial \xi}\left(G^{(1)}(\eta)\frac{\partial \overline{C}}{\partial \xi} + G^{(2)}(\eta)\frac{\partial^2 \overline{C}}{\partial \xi^2} + \cdots\right)} = 0 \tag{62}$$

which can be rewritten as follows:

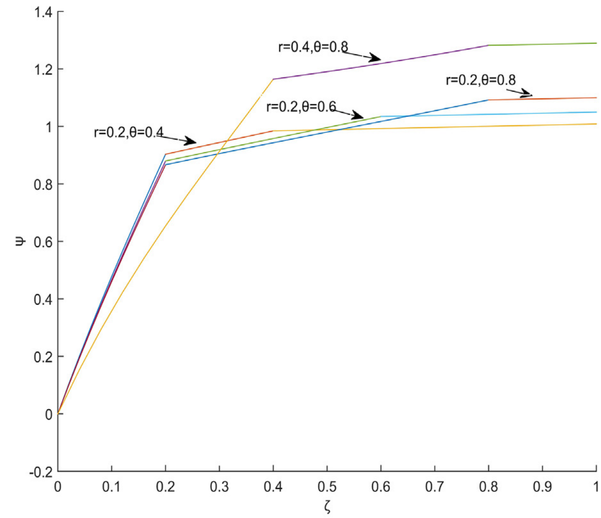

(a)

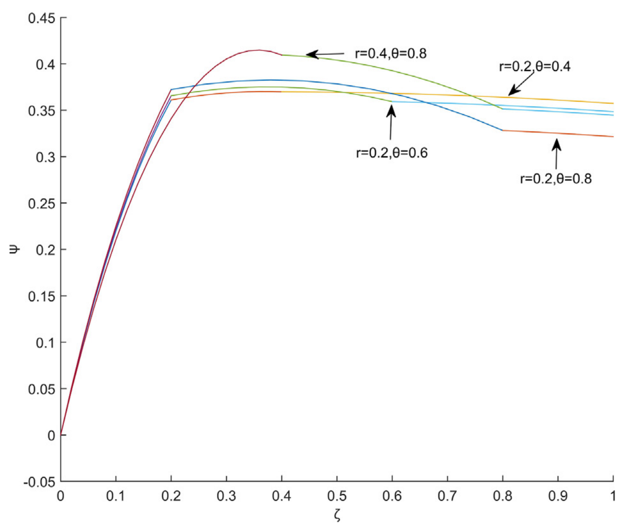

(b)

Fig. 7. Variation of ψ with ζ for $\alpha = 1.0$, $\boldsymbol{E_r} = 0.4$, $N_k = 1$, $M_1 = 10, M_2 = 1, M_3 = 1/10$: (a) $\omega = 1$ and (b) $\omega = -1$.

$$\frac{\partial \overline{C}}{\partial \tau} = (-\overline{\psi_\phi' G^{(1)}(\eta)})\frac{\partial^2 \overline{C}}{\partial \xi^2} + (-\overline{\psi_\phi' G^{(2)}(\eta)})\frac{\partial^3 \overline{C}}{\partial \xi^3} + \cdots \tag{63}$$

After completing the initial stage of the contaminant transport process in the three-layer wetland, the distribution of vertical average concentration can be considered as Gaussian distribution (Chatwin, 1970; Fischer et al., 1979; Taylor, 1953; Wu and Chen, 2012). As the third- and higher-order derivatives of the mean concentration can be neglected, the following dispersion model can be obtained:

$$\frac{\partial \overline{C}}{\partial \tau} = -\overline{\psi_\phi' G^{(1)}(\eta)}\frac{\partial^2 \overline{C}}{\partial \xi^2}. \tag{64}$$

To ascertain the unknown function, Eqs. (60) and (63) are substituted into Eq. (53) as follows:

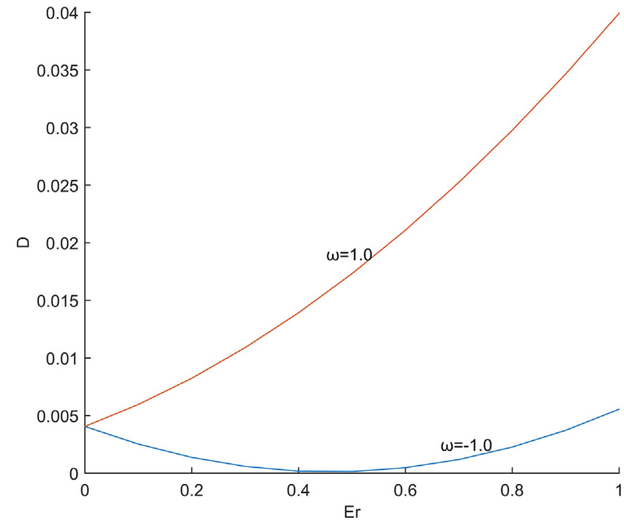

Fig. 8. Variation of D with $\boldsymbol{E_r}$ for $\alpha = 1.0, Pe_1 = Pe_2 = Pe_3 = 1, M_k = 1.0, N_k = 1.0, \phi_k = 0.5$, and $r = 1/3, \theta = 2/3$.

$$\begin{aligned}
&-\overline{\psi_\phi' G^{(1)}(\eta)}\left(\frac{\partial^2 \overline{C}}{\partial \xi^2} + G_k^{(1)}(\eta_k)\frac{\partial^3 \overline{C}}{\partial \xi^3} + \cdots\right) \\
&\quad + \psi_{\phi k}'\left(\frac{\partial \overline{C}}{\partial \xi} + G_k^{(1)}(\eta_k)\frac{\partial^2 \overline{C}}{\partial \xi^2} + G_k^{(1)}(\eta_k)\frac{\partial^3 \overline{C}}{\partial \xi^3} + \cdots\right) \\
&\quad = \frac{T_c}{T_k}\left(\frac{\partial^2 G_k^{(1)}(\eta_k)}{\partial \eta_k^2}\frac{\partial \overline{C}}{\partial \xi} + \frac{\partial^2 G_k^{(2)}(\eta_k)}{\partial \eta_k^2}\frac{\partial^2 \overline{C}}{\partial \xi^2} + \frac{\partial^2 G_k^{(3)}(\eta_k)}{\partial \eta_k^2}\frac{\partial^3 \overline{C}}{\partial \xi^3} + \cdots\right)
\end{aligned} \tag{65}$$

Comparing the term with the first derivative yields the following:

$$\psi_{\phi k}' = \frac{T_c}{T_k}\cdot\frac{\partial^2 G_k^{(1)}(\eta_k)}{\partial \eta_k^2}, k = 1,2,3 \tag{66}$$

Integrating Eq. (66) twice under the conditions of Eqs. (55)–(59) yields the following:

$$G_1^{(1)}(\eta_1) = \frac{T_1}{T_c}\int r^{\eta_1}\int 0^{\eta_1}\psi_{\phi_1}' d\eta_1 d\eta_1 + C_b \tag{67}$$

$$G_2^{(1)}(\eta_2) = \frac{T_2}{T_c}\left(\int_{\eta_2}^{r}\int_{\eta_2}^{\theta}\psi_{\phi_2}' d\eta_2 d\eta_2 + \int_{\eta_2}^{r}\int_{\theta}^{1}\psi_{\phi_3}' d\eta_3 d\eta_2\right) + C_b \tag{68}$$

and

$$G_3^{(1)}(\eta_3) = \frac{T_3}{T_c}\int_{\eta_3}^{r}\int_{\eta_3}^{1}\psi_{\phi_1}' d\eta_3 d\eta_3 + C_b \tag{69}$$

where C_b is a constant.

In the dimensional coordinate, Eq. (64) can be adapted as follows:

$$\frac{\partial \overline{C}}{\partial t} + \overline{u_\phi}\frac{\partial \overline{C}}{\partial x} = -\overline{\kappa\left(\lambda + \frac{K}{\phi}\right)\frac{Pe\cdot\psi_\phi'\cdot g^{(1)}(\eta)}{1/Pe}}\frac{\partial^2 \overline{C}}{\partial x^2} \tag{70}$$

where

$$Pe_k = \frac{Hu_c}{\kappa_k\left(\lambda_k + \frac{\kappa_k}{\phi_k}\right)}, k = 1,2,3 \tag{71}$$

Pe_k are *Peclet* numbers, and

$$g_1^{(1)}(\eta_1) = \int_{r}^{\eta_1}\int_{0}^{\theta}\psi_{\phi_1}' d\eta_1 d\eta_1 + C_b, \tag{72}$$

$$g_2^{(1)}(\eta_2) = \int_{\eta_2}^{r}\int_{\eta_2}^{\theta}\psi_{\phi_2}' d\eta_2 d\eta_2 + \int_{\eta_2}^{r}\int_{\theta}^{1}\psi_{\phi_3}' d\eta_3 d\eta_2 + C_b, \tag{73}$$

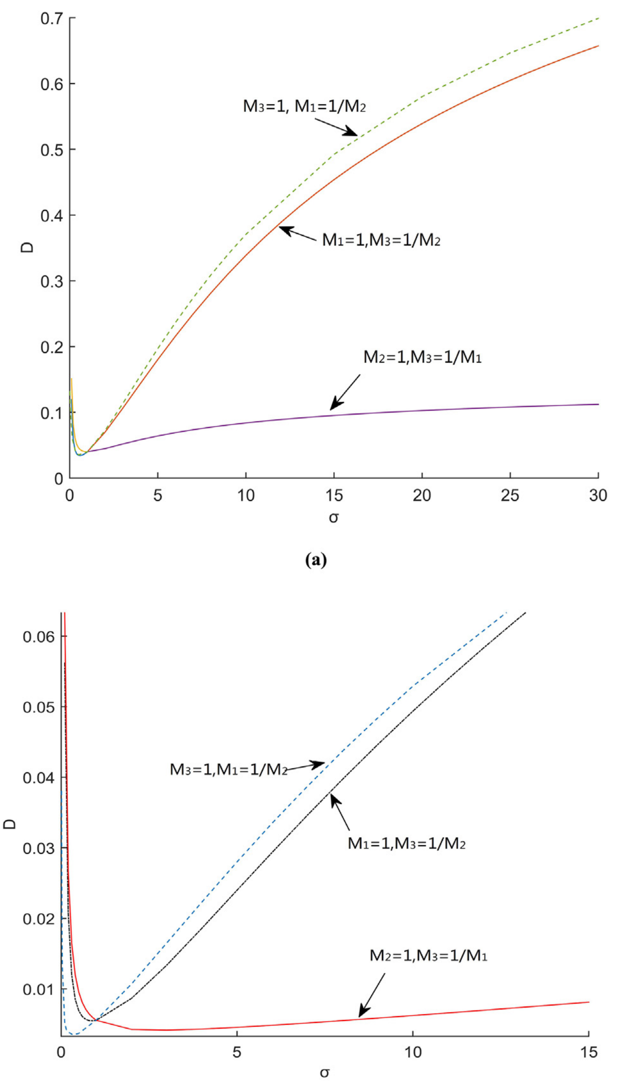

Fig. 9. Variation of D with M for $\boldsymbol{E_r} = 1.0$, $N_k = 1.0$, $\alpha = 1.0$, $\Phi_k = 0.5$, $Pe_k = 1.0$, $r = 1/3$, and $\theta = 2/3$: (a) $\omega = 1.0$ and (b) $\omega = -1.0$.

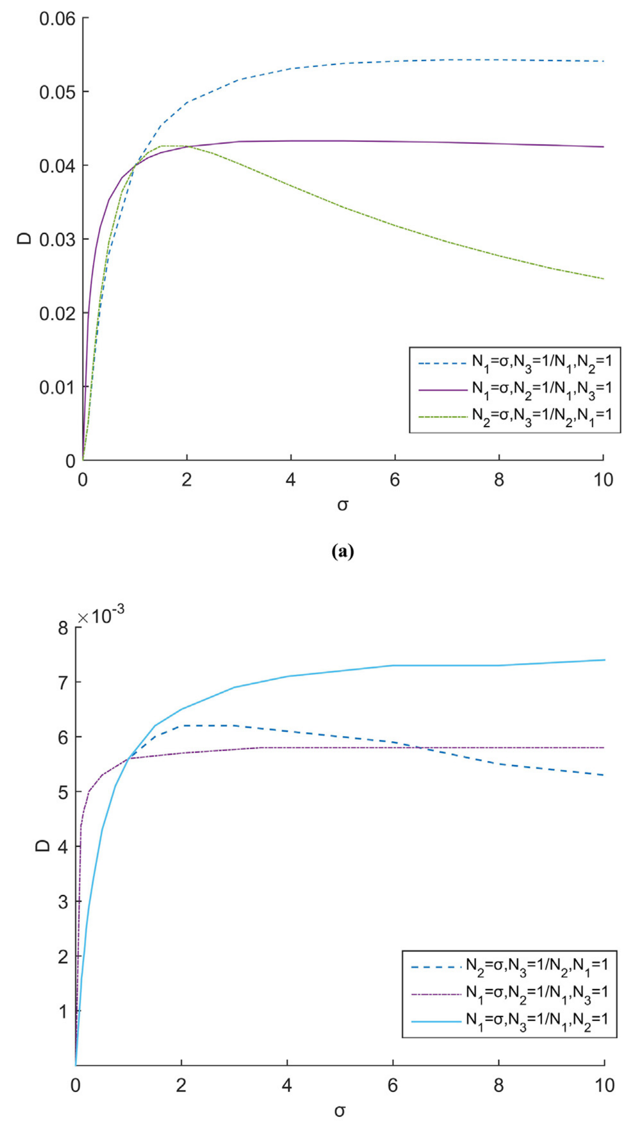

Fig. 10. Variation of D with N for $\boldsymbol{E_r} = 1.0$, $M_k = 1.0$, $\alpha = 1.0$, $\Phi_k = 0.5$, $Pe_k = 1.0$, $r = 1/3$, and $\theta = 2/3$: (a) $\omega = 1.0$ and (b) $\omega = -1.0$.

and

$$g_3^{(1)}(\eta_3) = \int_{\eta_3}^{r}\int_{\eta_3}^{1}\psi'_{\phi_3}d\eta_3 d\eta_3 + C_b, \tag{74}$$

where

$$\psi'_\phi = \psi_\phi - \overline{\psi}_\phi \tag{75}$$

and

$$\begin{aligned}\overline{\psi}_\phi = {} & \frac{\theta-r}{\alpha^2 N_2\phi_2} + \frac{1-\theta}{\alpha^2 N_3\phi_3} + \frac{1}{\alpha^2 N_1\phi_1} + \frac{1}{\alpha\sqrt{M_3N_3}\phi_3}\left[C_5(\sigma_1-\sigma_4)\right.\\ & \left. + C_6\left(\frac{1}{\sigma_1}-\frac{1}{\sigma_4}\right)\right] + \frac{1}{\alpha\sqrt{M_1N_1}\phi_1}\left[C_1(\sigma_3-1)-C_2\left(\frac{1}{\sigma_3}-1\right)\right]\\ & + \frac{1}{\alpha\sqrt{M_2N_2}\phi_2}\left[C_3(\sigma_5-\sigma_2)-C_4\left(\frac{1}{\sigma_5}-\frac{1}{\sigma_2}\right)\right]\end{aligned} \tag{76}$$

when $t^* = t, \zeta = x - \overline{u_\phi}t$, Eq. (70) can be rewritten as follows:

$$\frac{\partial\overline{C}}{\partial t^*} = D_T\cdot\frac{\partial^2\overline{C}}{\partial\zeta^2} \tag{77}$$

where

$$D_T = -\overline{\kappa\left(\lambda + \frac{K}{\phi}\right)}\frac{\overline{Pe\cdot\psi'_\phi\cdot g^{(1)}(\eta)}}{\overline{1/Pe}} \tag{78}$$

can be termed as the Taylor dispersivity. Obviously, the solute cloud moves downstream along with the mean flow velocity.

The initial and boundary conditions can be written as

$$\overline{C(\zeta,t^*)}|_{\zeta=\pm\infty} = 0 \tag{79}$$

and

$$\overline{C(\zeta,t^*)}|_{t^*=0} = \frac{Q\delta(\zeta)}{H}\cdot\overline{1/\phi} \tag{80}$$

where

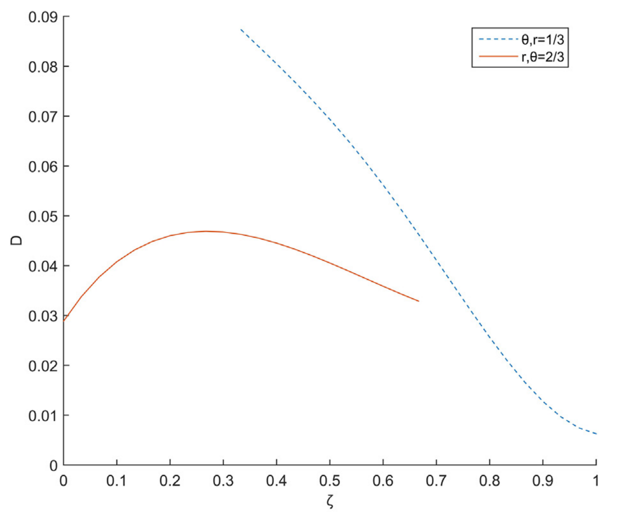

(a)

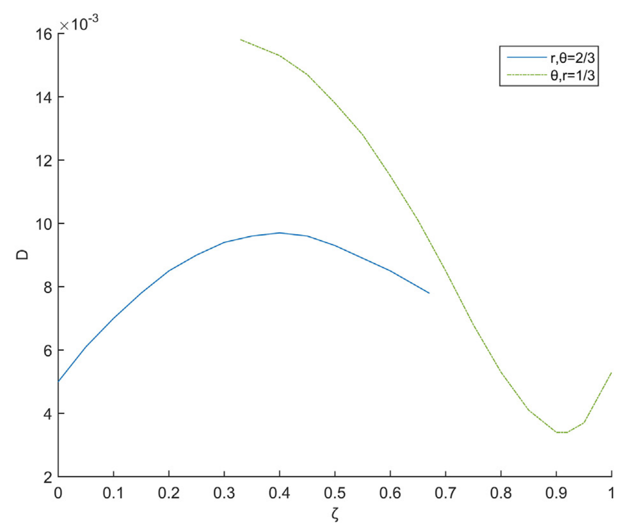

(b)

Fig. 11. Variation of D with r and θ for $\boldsymbol{E_r} = 1.0$, M_1:M_2:M_3 = 1:2:4, $N_k = 1.0$, $\alpha = 1.0$, $\Phi_k = 0.5$, $Pe_k = 1.0$: (a) $\omega = 1.0$ and (b) $\omega = -1.0$.

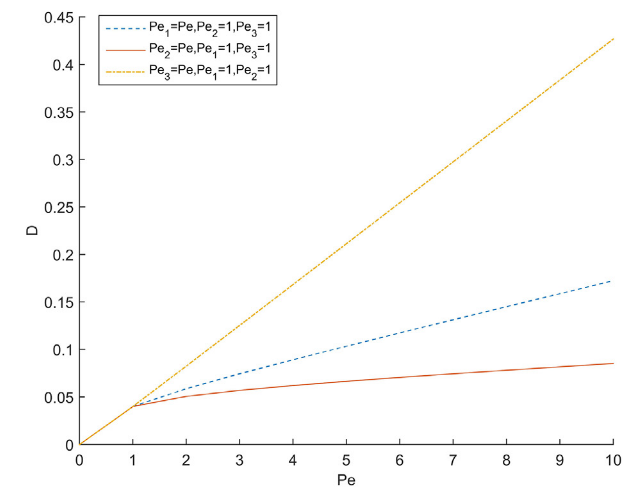

(a)

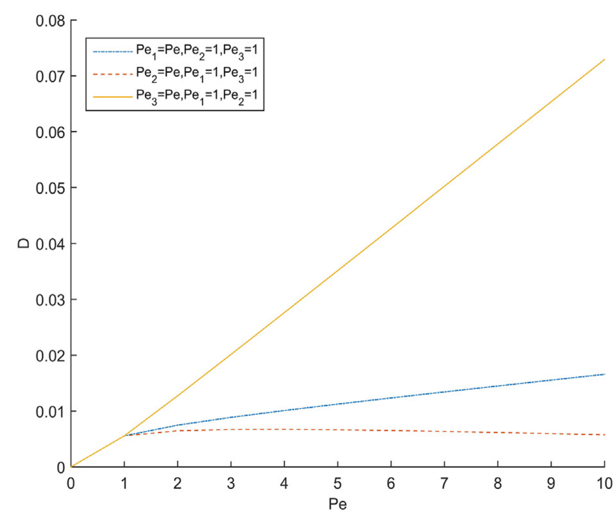

(b)

Fig. 12. Variation of D with Pe for $\boldsymbol{E_r} = 1.0$, $M_k = 1.0$, $N_k = 1.0$, $\alpha = 1.0$, $\Phi_k = 0.5$, $r = 1/3$, and $\theta = 2/3$: (a) $\omega = 1.0$ and (b) $\omega = -1.0$.

$$\overline{1/\phi} = \frac{r}{\phi_1} + \frac{\theta - r}{\phi_2} + \frac{1-\theta}{\phi_3} \tag{81}$$

The following analytical solution under environmental dispersion for mean concentration evolution is obtained:

$$\overline{C(\zeta,t^*)} = \frac{Q\cdot\overline{1/\phi}}{H\sqrt{4\pi D_T t^*}}\cdot\exp\left(-\frac{\zeta^2}{4D_T t^*}\right) \tag{82}$$

Afterward, we obtain the following:

$$S = 4\sqrt{-D_T t^* \ln\frac{C_0 H\sqrt{4\pi D_T t^*}}{Q\cdot\overline{1/\phi}}} \tag{83}$$

Ecological degradation, which may be the consequence of absorption, hydrolysis, bacteria metabolism, and assimilation plants, should be considered when investigating the contaminant transport process in three-layer wetlands under the influence of wind (US EPA, 1999). The source term $-\phi k_a C$ is incorporated into the solution to assess the effects of ecology. After determining the mean concentration under hydraulic and ecological effects, we obtain the following:

$$\overline{C_e(\zeta,t^*)} = \frac{Q\cdot\overline{1/\phi}}{H\sqrt{4\pi D_T t^*}}\cdot\exp\left(-k_a t^* - \frac{\zeta^2}{4D_T t^*}\right) \tag{84}$$

where $k_a(s^{-1})$ is the apparent reaction rate.

The critical length of the region influenced by the contaminant can be obtained as follows while considering both the ecological and hydraulic effects:

$$S_e = 4\sqrt{-D_T t^*\left(k_a t^* + \ln\frac{C_0 H\sqrt{4\pi D_T t}}{Q\cdot\overline{1/\phi}}\right)} \tag{85}$$

4. Dispersivity

To determine the environmental dispersion, we define the

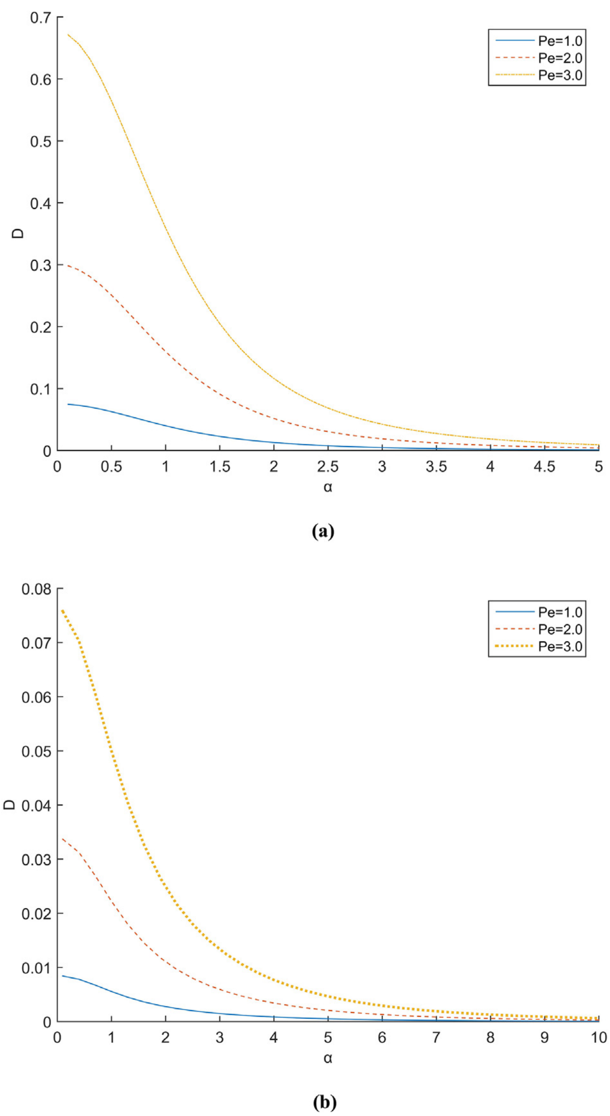

Fig. 13. Variation of D with α for $Pe_k = Pe$, $\boldsymbol{E_r} = 1.0$, $M_k = 1.0$, $N_k = 1.0$, $\alpha = 1.0$, $\Phi_k = 0.5$, r = 1/3, and $\theta = 2/3$: (a) $\omega = 1.0$ and (b) $\omega = -1.0$.

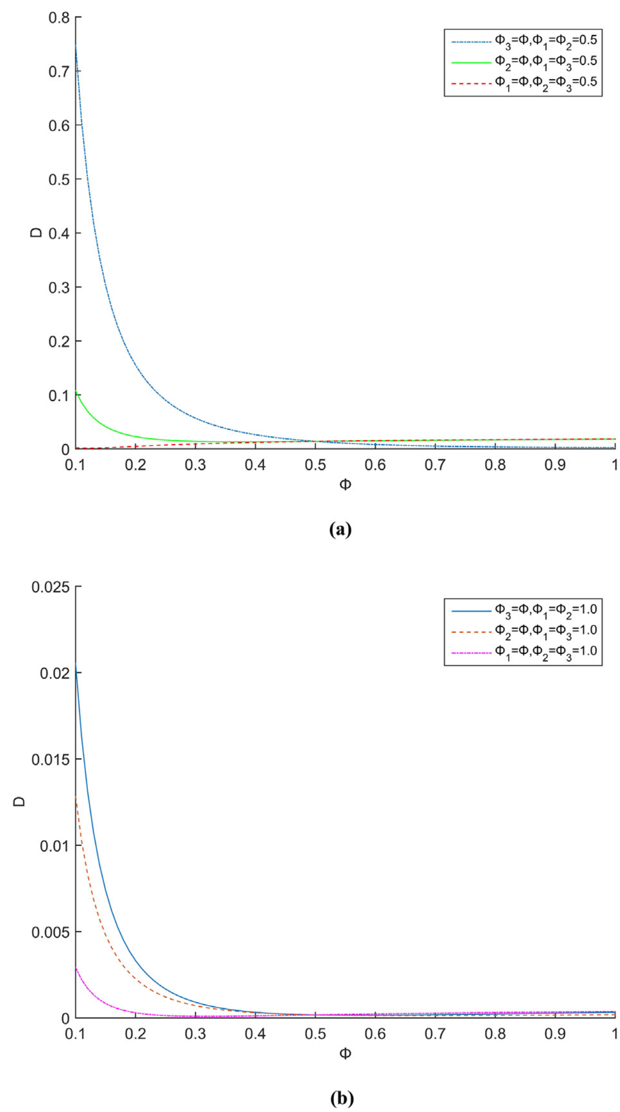

Fig. 14. Variation of D with Φ for $Pe_k = 1$, $\boldsymbol{E_r} = 1.0$, $M_k = 1.0$, $N_k = 1.0$, $\alpha = 1.0$, $r = 1/3$, and $\theta = 2/3$: (a) $\omega = 1.0$ and (b) $\omega = -1.0$.

following:

$$D = -\frac{\overline{Pe\cdot g^{(1)}(\eta)\cdot\psi'_{\phi}}}{\overline{1/Pe}} = -\frac{1}{r/Pe_1 + (\theta-r)/Pe_2 + (1-\theta)/Pe_3}\left(Pe_1\int_0^r g_1^{(1)}(\eta_1)\cdot\psi'_{\phi_1}d\eta_1 + Pe_2\int_r^\theta g_2^{(1)}(\eta_2)\cdot\psi'_{\phi_2}d\eta_2 + Pe_3\int_\theta^1 g_3^{(1)}(\eta_3)\cdot\psi'_{\phi_3}d\eta_3\right) \tag{86}$$

Appendix B presents a detailed expression of each integral term.

To assess the contaminant transport process, Figs. 8 to 14 plot the dispersivity D against the characteristic parameters $\boldsymbol{E_r}$, M, N, α, Pe, Φ, r, and θ for $\omega = 1.0$ and $\omega = -1.0$. The results in Fig. 8 are consistent with those in Zeng et al. (2012). D increases along with $\boldsymbol{E_r}$ when $\omega = 1.0$, and initially decreases to the minimum and then subsequently increases along with $\boldsymbol{E_r}$ when $\omega = -1.0$. Figs. 9 and 10 present the environmental dispersivity D changing with M and N. The dispersivity D has a significantly smaller value when $\omega = -1.0$ than when $\omega = 1.0$. In both cases, the value of D initially decreases and reaches the minimum value, then it increases as M increases. By contrast, the relevance of dispersivity to N shows opposite characteristics that the value of D increases to the maximum value first and then decreases as N increases. This finding implies that M and N are relative parameters. Given that the depth of the three-layer wetland does not contribute to dispersivity with the identical parameters of each layer, Fig. 11 shows the dependence of dispersivity on r and θ when M_1:M_2:M_3 = 1:2:4. Fig. 12 shows the influence of Pe on the variation of dispersivity. In Fig. 12(a) and (b), the three *Peclet* numbers are positively associated with D, and the separate *Peclet* numbers in each layer produce a nearly linear effect on the variation of dispersivity. As shown in Fig. 13, given the unified Pe in the three-layer wetland, the dependence of dispersivity on Pe follows the quadratic law. The value of D rapidly decreases along with increasing α, and then reaches a value close to zero. Therefore, the characteristic parameter α negatively affects environmental dispersion. Fig. 14 demonstrates the effect of porosity on environmental dispersion. In both cases, the effect of Φ_3 and Φ_2 initially demonstrates a downward trend, and then remains steady under the weak condition similar to the effect of $\Phi 1$.

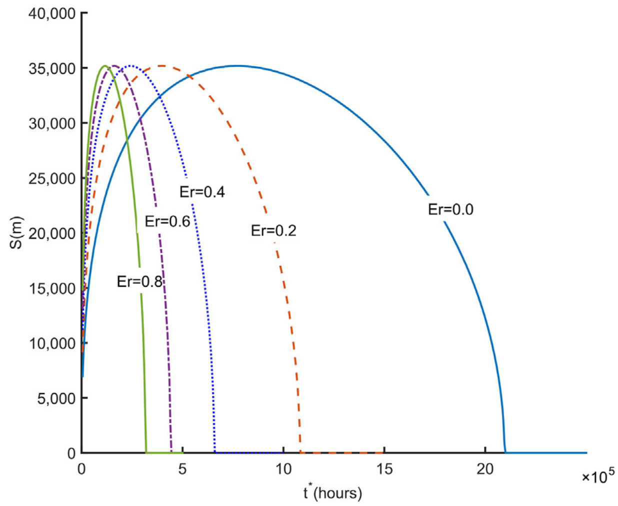

(a)

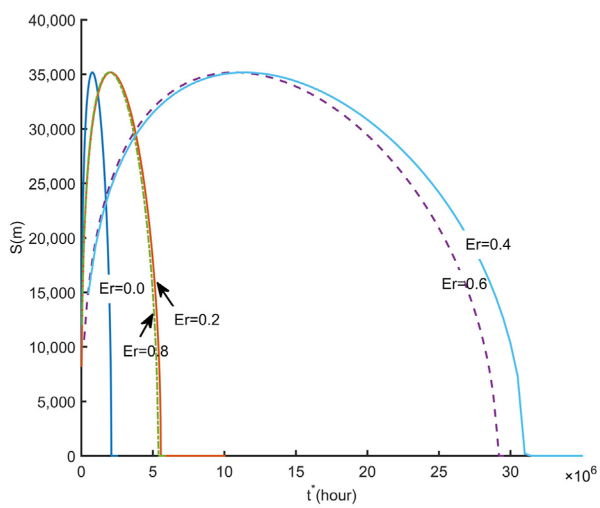

(b)

Fig. 15. Variation of S for E_r = 0.0, 0.2, 0.4, 0.6, and 0.8 with t^*; (a) ω = 1.0 and (b) ω = −1.0.

Table 1
Duration of the contaminant cloud for Pb.

ω	t^*(h)				
	E_r = 0.0	E_r = 0.2	E_r = 0.4	E_r = 0.6	E_r = 0.8
1.0	2.10E+06	1.10E+06	6.60E+05	4.45E+05	3.20E+05
−1.0	2.10E+06	5.56E+06	3.12E+07	2.92E+07	5.40E+06

5. Applications

Considering the instantaneous emission of contaminants into the three-layer wetland, we observe that the region influenced by the contaminant is formed. As such, the maximum critical length and duration of the affected region must be analyzed. Plumbum (Pb) is a common heavy metal in wetlands with a safe upper limit C_0 of 5.0×10^{-5} kg m^{-3} under category III of the National Standard of the People's Republic of China (GB3838-2002) (CN EPA and CN GAQSIQ, 2002).

Given the high porosity of the system, the tortuosity of Pb can be calculated as follows using the equation of Bruggeman (Liu and Masliyah, 2005):

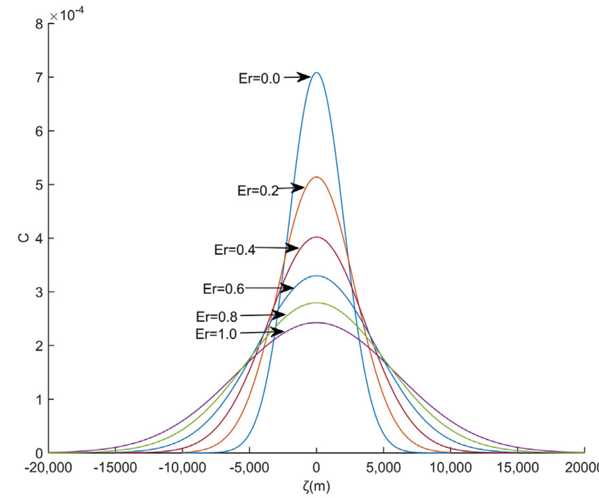

(a)

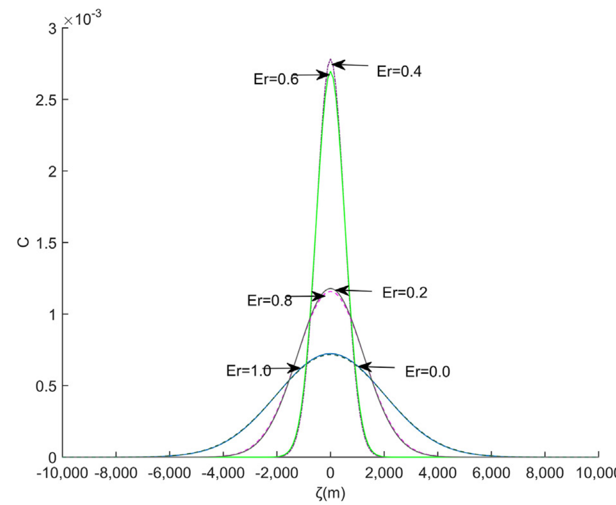

(b)

Fig. 16. Variation of $\overline{C}$ with ζ at t = 10000 h; (a) ω = 1.0 and (b) ω = 1.0.

Table 2
Safe upper limits of concentration according to National Standard of the People's Republic of China (GB 3838-2002) for COD, BOD_5, TN, TP, Pb.

Constituents	Five standards for safe upper limits of concentration				
	I (mg L^{-1})	II (mg L^{-1})	III (mg L^{-1})	IV (mg L^{-1})	V (mg L^{-1})
COD	15.0	15.0	20.0	30.0	40.0
BOD_5	3.0	3.0	4.0	6.0	10.0
TN	0.20	0.50	1.0	1.50	2.0
TP	0.02	0.10	0.20	0.30	0.40
Pb	0.01	0.01	0.05	0.05	0.10

Table 3
Duration of the contaminant cloud for Pb, TP, TN, BOD_5, and COD with E_r = 0.8.

Constituents	Duration of influenced region				
	I(h)	II(h)	III(h)	IV(h)	V(h)
COD	3.40E+00	3.40E+00	2.00E+00	8.60E−01	4.80E−01
BOD_5	8.40E+01	8.40E+01	5.00E+01	2.20E+01	7.59E+00
TN	1.89E+04	3.20E+03	7.56E+02	3.36E+02	1.91E+02
TP	1.89E+06	7.58E+04	2.00E+04	8.60E+03	4.80E+03
Pb	7.58E+06	7.58E+06	3.20E+05	3.20E+05	7.58E+04

Table 4
Maximal critical length of the contaminant cloud for Pb, TP, TN, BOD_5, and COD with $\boldsymbol{E_r} = 0.8$.

Constituents	Maximum length of influenced region				
	I(m)	II(m)	III(m)	IV(m)	V(m)
COD	1.17E+02	1.17E+02	8.79E+01	5.86E+01	4.40E+01
BOD_5	5.86E+02	5.86E+02	4.40E+02	2.93E+02	1.76E+02
TN	8.79E+03	3.51E+03	1.76E+03	1.73E+03	8.79E+02
TP	8.79E+04	1.76E+04	8.79E+03	5.86E+03	4.40E+03
Pb	1.76E+05	1.76E+05	3.52E+04	3.52E+04	1.76E+04

$$\kappa = \sqrt{\phi}.$$

Following the equation of Ergun (1952), the shear factor F can be calculated as follows:

$$F = \frac{150(1-\phi)^2}{d^2\phi^3}.$$

The properties of ambient water are calculated as $\rho = 1.0 \times 10^3 kg/m^3$, $\mu = 1.0 \times 10^{-3} kgm^{-1}s^{-1}$, and $\lambda = 1.0 \times 10^{-5} m^2 s^{-1}$ (Lightbody and Nepf, 2006). *Peclet* and *Reynolds* numbers are defined as $Pe_d = \bar{u}d/\lambda$ and $Re_d = \bar{u}d\rho/\mu$ respectively. The vertical momentum dispersivity **L** and vertical concentration dispersivity **K** can be expressed as follows (Liu and Masliyah, 2005):

$$\mathbf{L} = 160 Re_d \mu \phi^{11/3}(1-\phi)^{2/3}\left[4.0 + \frac{25Re_d}{(100 + Re_d)(1 + 2 \times 10^{-6} Re_d)}\right]^{-1}$$

and

$$\mathbf{K} = 160 Pe_d \lambda \phi^{11/3}(1-\phi)^{2/3}\left[4.0 + \frac{25Pe_d}{(100 + Pe_d)(1 + 2 \times 10^{-6} Pe_d)}\right]^{-1}.$$

The characteristic parameters of the wetland flow include $\phi_1 = \phi_2 = 0.9$ (US EPA, 1999), $\phi_3 = 0.945$ (Stone and Shen, 2002), $d_1 = 2.0 \times 10^{-2} m$ (Nepf and Ghisalberti, 2008), $d_2 = 1.0 \times 10^{-2} m$ (Mitsch and Gosselink, 1993), $d_3 = 0.635 \times 10^{-2}$ (Stone and Shen, 2002), $H = 0.3m$, $r = 1/3$, $\theta = 2/3$ (US EPA, 1999), and $\bar{u} = 0.15 m/s$ (Stone and Shen, 2002).

Given the instantaneous emission of $Q = 1\,\mathrm{kg\,m^{-1}}$ and $ka = 1.11 \times 10^{-6}\,\mathrm{s^{-1}}$ (Zeng and Chen, 2011), the variation of S with $t*$ for the three-layer wetland under the effect of wind is illustrated in Fig. 15, while its duration is presented in Table 1.

As shown in the Fig. 15, when $\omega = 1.0$, the duration of the contaminant cloud is extended along with increasing $\boldsymbol{E_r}$, which indicates that the wind enhances the dispersivity when $\omega = 1.0$. When $\omega = -1.0$, the wind makes the dispersivity complex, and the moderate $\boldsymbol{E_r}$ increases t most. The maximum critical length is almost equal in both cases. The duration and maximal critical length under the ideal condition $\boldsymbol{E_r} = 0$ are almost the same as those of the contaminant dispersion in a three-layer wetland with no wind under an identical ambient environment (Wang et al., 2013).

As shown in the Fig. 16, the maximum of $\overline{C}$ decreases along with increasing $\boldsymbol{E_r}$ in the first case ($\omega = 1$), which implies that the wind positively affects the dispersion of flow. In the second case, the regulation is analogous to that shown in Fig. 16(b), that is, the moderate *Er* greatly weakens the dispersion.

Tables 3 and 4 show the effect of the five typical contaminant constituents (i.e., Pb, TP, TN, BOD_5, and COD) on the duration and maximal critical length of the contaminant cloud with $\boldsymbol{E_r} = 0.8$ under five water-quality standards of category of the National Standard of the People's Republic of China, as is illustrated in Table 2.

As illustrated in the Fig. 17, given the same time emission of five different contaminants (COD, BOD_5, TN, TP, Pb) into the three-layer wetland under each water-quality standards, the contaminant Pb causes the greatest effect on both duration and critical length of the contaminant cloud.

6. Conclusions

Given that the wind can affect the dispersion of flow in three-layer wetlands, the velocity profile and solute dispersion are analyzed in this paper while considering the effects of heterogeneity, ecological degradation and wind.

The analytical solution of velocity is formulated while considering a fully developed steady flow in the three-layer wetland under the effect of wind. Our study revealed that depth, viscous friction, heterogeneity, wind force, and ecological degradation can all affect environmental dispersion to some extent.

We simplify the calculation process by adopting theory of asymptotic analysis to analyze the contaminant dispersivity instead of the concentration moments method. A basic formula for dispersion in a three-layer wetland under the effect of wind is obtained by vertically averaging the concentration transport equations. Following Gill, the unknown terms are closed by a mean concentration expansion. The characteristic of dispersivity is obtained with the dimensionless parameters of the influenced region. By considering both ecological degradation and hydraulic effects, we obtain the analytical solutions for the mean concentration and critical lengths of the contaminant cloud under the effect of wind.

This paper also provides indicators to environmental assessment. As illustrated in the applications, the duration and maximum length of region influenced by five contaminant constituents are given under different water-quality standards. These results prove that the effect of wind may change the duration and maximal critical length of the flow greatly in a three-layer wetland.

Acknowledgments

This work was financially supported by the Key Program of National Natural Science Foundation of China (No. 51439007), and Natural Science Foundation of China (No. 11672213).

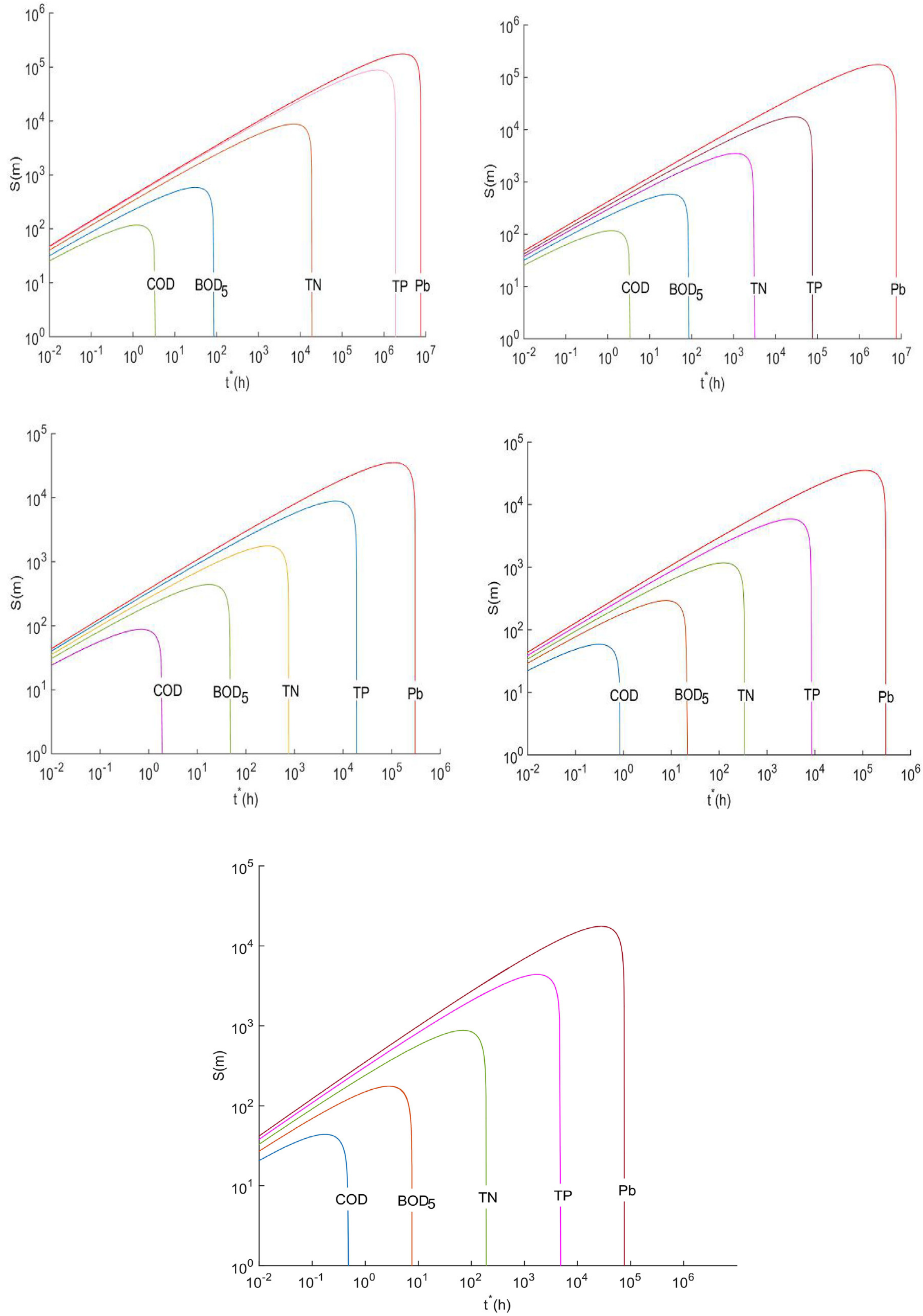

Fig. 17. Variation of *S* for COD, BOD_5, TN, TP and Pb under five water quality standards (I, II, III, IV, V).

Appendix A

$$\Omega_1 = -\frac{A_1}{B_1},$$
$$\Omega_2 = -\frac{A_2}{B_2},$$
$$\Omega_3 = \frac{A_3}{B_3},$$
$$\Omega_4 = -\frac{A_4}{B_4},$$
$$\Omega_5 = \frac{A_5}{B_5},$$
$$\Omega_6 = \frac{A_6}{B_6},$$
$$l_1 = \sqrt{\frac{N_1}{M_1}},$$
$$l_2 = \sqrt{\frac{N_2}{M_2}},$$
$$l_3 = \sqrt{\frac{N_3}{M_3}}$$

where

$$A_1 = 2\sigma_6^2(\sigma_9\sigma_5-\sigma_9\sigma_7+\sigma_4\sigma_5-\sigma_7\sigma_5)\sinh\left(\frac{\sigma_{11}}{2}\right)-\frac{N_1 l_3}{N_2 l_3}(\sigma_4\sigma_5\sigma_6+\sigma_7\sigma_5\sigma_6+\sigma_1\sigma_6\sigma_4\sigma_9-\sigma_1\sigma_6\sigma_4\sigma_{10}-\sigma_9\sigma_5\sigma_6-\sigma_9\sigma_7\sigma_6)-\frac{N_1}{l_2\sqrt{M_3N_3}}\sigma_1\sigma_6\sigma_4(\sigma_9-\sigma_{10})$$
$$+\frac{l_3}{l_2}2\sigma_6^{0.5}(\sigma_9\sigma_5-\sigma_9\sigma_7+\sigma_4\sigma_5-\sigma_7\sigma_5)+\frac{l_1l_3}{l_2^2}(\sigma_9\sigma_5-\sigma_9\sigma_7-\sigma_4\sigma_5+\sigma_7\sigma_5)-\frac{N_1}{N_2}\sigma_6(\sigma_4\sigma_5-\sigma_7\sigma_5+\sigma_9\sigma_5-\sigma_9\sigma_7)+\frac{l_1}{l_2}(\sigma_9\sigma_5+\sigma_9\sigma_7+\sigma_4\sigma_5+\sigma_7\sigma_5)$$
$$-4Er\alpha\omega\frac{N_1}{l_2}\sigma_1\sigma_2\sigma_3^{0.5}\sigma_5^{0.5}\sigma_6$$

$$B_1 = N_1 2a^2\sigma_6\sinh(\sigma_{11})(\sigma_9\sigma_5-\sigma_9\sigma_7+\sigma_4\sigma_5-\sigma_7\sigma_5)+\frac{N_1l_1}{l_2}2a^2\sigma_6\cosh(\sigma_{11})(\sigma_9\sigma_5+\sigma_9\sigma_7+\sigma_4\sigma_5+\sigma_7\sigma_5)\frac{M_2N_1l_1l_3}{N_2}2a^2\sigma_6\cosh(\sigma_{11})(\sigma_9\sigma_5-\sigma_9\sigma_7-\sigma_4\sigma_5+\sigma_7\sigma_5)$$
$$+\frac{N_1}{M_3N_2}2a^2\sigma_6\sinh(\sigma_{11})(\sigma_9\sigma_5+\sigma_9\sigma_7-\sigma_4\sigma_5-\sigma_7\sigma_5)$$

$$A_2 = 2\sigma_6^{1.5}(\sigma_9\sigma_5-\sigma_9\sigma_7+\sigma_4\sigma_5-\sigma_7\sigma_5)\sinh\left(\frac{\sigma_{11}}{2}\right)-\frac{N_1l_3}{N_2l_2}(\sigma_4\sigma_5\sigma_6+\sigma_7\sigma_5\sigma_6+\sigma_9\sigma_4\sigma_6\sigma_1-\sigma_{10}\sigma_4\sigma_6\sigma_1-\sigma_9\sigma_5\sigma_6-\sigma_9\sigma_7\sigma_6)+\frac{l_1}{l_2}\sigma_6^2(\sigma_4\sigma_5+\sigma_7\sigma_5+\sigma_9\sigma_5+\sigma_9\sigma_7)$$
$$+\frac{N_1}{l_2\sqrt{M_3N_3}}\sigma_8\sigma_6\sigma_1(\sigma_9-\sigma_{10})+\frac{l_3}{l_2}2\sigma_6^{1.5}\sinh\left(\frac{\sigma_{11}}{2}\right)(\sigma_9\sigma_5+\sigma_9\sigma_7-\sigma_4\sigma_5-\sigma_7\sigma_5)+\frac{N_1}{N_2}\sigma_6(\sigma_4\sigma_5-\sigma_7\sigma_5+\sigma_9\sigma_5-\sigma_9\sigma_7)-\frac{l_1l_3}{l_2^2}\sigma_6^2(\sigma_4\sigma_5-\sigma_7\sigma_5-\sigma_9\sigma_5+\sigma_9\sigma_7)$$
$$+4Er\alpha\omega\frac{N_1}{l_2}\sigma_1\sigma_2\sigma_6\sigma_3^{0.5}\sigma_5^{0.5}$$

$$B_2 = N_1 2a^2\sigma_6\sinh(\sigma_{11})(\sigma_9\sigma_5-\sigma_9\sigma_7+\sigma_4\sigma_5-\sigma_7\sigma_5)+\frac{N_{1l_1}}{l_2}2a^2\sigma_6\cosh(\sigma_{11})(\sigma_9\sigma_5+\sigma_9\sigma_7+\sigma_4\sigma_5+\sigma_7\sigma_5)+\frac{M_2N_1l_1l_3}{N_2}2a^2\sigma_6\cosh(\sigma_{11})(\sigma_9\sigma_5-\sigma_9\sigma_7-\sigma_4\sigma_5+\sigma_7\sigma_5)$$
$$+\frac{N_1}{M_3N_2}2a^2\sigma_6\sinh(\sigma_{11})(\sigma_9\sigma_5+\sigma_9\sigma_7-\sigma_4\sigma_5-\sigma_7\sigma_5)$$

$$A_3 = 2Er\omega\sigma_2\sigma_3\sigma_5^{0.5}\left(\frac{l_1}{l_2^2}(\sigma_6^2+1)-\frac{1}{l_2}(1-\sigma_6^2)\right)-\frac{l_1}{l_2^2\sqrt{M_3N_3}}\sigma_2(\sigma_5-\sigma_3^2)(1+\sigma_6^2)+\left(\frac{1}{l_2\sqrt{M_3N_3}}-\frac{l_3}{l_2N_2}\right)\sigma_2(\sigma_5-\sigma_3^2)(1-\sigma_6^2)+\frac{1}{\sqrt{M_1N_1}\,l_2}\sigma_1(\sigma_3^2+\sigma_5)(\sigma_6-1)^2$$
$$+\frac{l_3}{l_2^2\sqrt{M_1N_1}}\sigma_1(\sigma_5-\sigma_3^2)(1-\sigma_6)^2+\frac{l_1l_3}{l_2^2N_2}(\sigma_5-\sigma_3^2)(\sigma_2-\sigma_1)(1+\sigma_6^2)-\frac{l_1}{l_2N_2}\sigma_1(\sigma_5+\sigma_6^2)(1+\sigma_6^2)$$

$$B_3 = a((\sigma_7-\sigma_4)(\sigma_5+\sigma_3^2)(1-\sigma_6^2)+\frac{l_1}{l_2}(\sigma_7+\sigma_4)(\sigma_5+\sigma_3^2)(1+\sigma_6^2)+\frac{l_2l_3}{l_2^2}(\sigma_7-\sigma_4)(\sigma_5-\sigma_3^2)(1+\sigma_6^2)+\frac{l_3}{l_2}(\sigma_7+\sigma_4)(\sigma_5-\sigma_3^2)(1-\sigma_6^2))$$

$$A_4 = \frac{l_1}{l_2^2}2Er\omega\sigma_2\sigma_3\sigma_5^{0.5}\sigma_7(1+\sigma_6^2)+\frac{1}{l_2}2Er\omega\sigma_2\sigma_3\sigma_5^{0.5}\sigma_7(1-\sigma_6^2)+\frac{l_1}{l_2N_2}\sigma_4\sigma_1(\sigma_5+\sigma_3^2)(1+\sigma_6^2)-\frac{l_1}{l_2^2\sqrt{M_3N_3}}\sigma_2\sigma_7(\sigma_5-\sigma_3^2)(1+\sigma_6^2)$$
$$-\left(\frac{1}{l_2\sqrt{M_3N_3}}-\frac{l_3}{l_2N_2}\right)\sigma_2\sigma_7(\sigma_5-\sigma_3^2)(1-\sigma_6^2)+\frac{l_1l_3}{l_2^2N_2}(\sigma_5-\sigma_3^2)(\sigma_2\sigma_7-\sigma_4\sigma_1)(\sigma_6^2+1)-\frac{M_2}{\sqrt{M_1N_1N_2}}\sigma_1\sigma_4((1+\sigma_6^2)(\sigma_5+\sigma_3^2)-2\sigma_3(\sigma_6+\sigma_5))$$
$$+\frac{l_3}{\sqrt{M_1N_1}\,l_2^2}(\sigma_1\sigma_4(1+\sigma_6^2)(\sigma_5-\sigma_3^2)+2\sigma_1\sigma_3^2\sigma_4(\sigma_6-\sigma_5))$$

$$B_4 = a((\sigma_7-\sigma_4)(\sigma_3^2+\sigma_5)(1+\sigma_6^2)+\frac{l_1}{l_2}(\sigma_7+\sigma_4)(\sigma_3^2+\sigma_5)(1+\sigma_6^2)+\frac{l_1l_3}{l_2^2}(1+\sigma_6^2)(\sigma_3^2-\sigma_5)(\sigma_4-\sigma_7)+\frac{l_3}{l_2}(1-\sigma_6^2)(\sigma_7+\sigma_4)(\sigma_5-\sigma_3^2)$$

$$A_5 = \left(\frac{N_2}{l_3} - \sqrt{M_3N_3}\right)\sigma_5^{0.5}(1-\sigma_6^2)(\sigma_2^2-\sigma_7) - M_3N_2 Er\alpha\omega\sigma_3^{0.5}(1-\sigma_6^2)(\sigma_2^2-\sigma_7) - \frac{l_1\sqrt{M_2N_2}}{N_3}\sigma_2(1+\sigma_1)(\sigma_5+\sigma_6^2) + \frac{l_1\sqrt{M_3N_3}}{l_2}(1+\sigma_6^2)(\sigma_2^2+\sigma_7-2\sigma_1\sigma_2)\sigma_5^{0.5}$$
$$+ \frac{1}{M_1N_1}2\sigma_5^{0.5}\sigma_1\sigma_2(1-\sigma_6)^2 + M_3 l_1\sqrt{M_2N_2}Er\alpha\omega\sigma_3^{0.5}(1+\sigma_6^2)(\sigma_2^2+\sigma_7) + \frac{M_2\sqrt{M_3}}{\sqrt{M_1N_1}}Er\alpha\omega\sigma_3^{0.5}(1+\sigma_6^2)(\sigma_2^2-\sigma_7) - \frac{1}{\sqrt{M_1N_1}}Er\alpha\omega\sigma_3^{0.5}(1-\sigma_6^2)(\sigma_2^2+\sigma_7)$$

$$B_5 = a^2(M_2N_3l_1(1+\sigma_6^2)(\sigma_5-\sigma_3)(\sigma_7-\sigma_2^2) + N_3\sqrt{M_2N_2}(\sigma_7+\sigma_2^2)(\sigma_5-\sigma_3)(1-\sigma_6^2)N_2\sqrt{M_3N_3}(1+\sigma_6^2)(\sigma_7-\sigma_2^2)(\sigma_5+\sigma_3) + \frac{l_1}{\sqrt{M_1N_1}}(1+\sigma_6^2)(\sigma_7+\sigma_2^2)(\sigma_5+\sigma_3)$$

$$A_6 = \left(\frac{N_2}{l_3}-\sqrt{M_3N_3}\right)\sigma_3\sigma_5^{0.5}(1-\sigma_6^2)(\sigma_4-\sigma_7) - \frac{l_1\sqrt{M_2N_2}}{N_3}\sigma_5^{0.5}\sigma_3(1+\sigma_6^2)(\sigma_4+\sigma_7) + \frac{1}{M_1N_1}2(1-\sigma_6)^2 + \frac{1}{M_1N_2}2((1+\sigma_6)^2-\sigma_5^{0.5}\sigma_1\sigma_2\sigma_3(1+\sigma_6^2))$$
$$+ M_3N_2Er\alpha\omega\sigma_3^{0.5}\sigma_5(1-\sigma_6^2)(\sigma_4-\sigma_7) - l_1M_3\sqrt{M_2N_2}Er\alpha\omega\sigma_3^{0.5}\sigma_5(1+\sigma_6^2)(\sigma_4+\sigma_7) + l_1M_2\sqrt{M_3N_3}Er\alpha\omega\sigma_3^{0.5}\sigma_5(1-\sigma_6^2)(\sigma_4-\sigma_7)$$
$$-\frac{1}{M_1N_1}Er\alpha\omega\sigma_3^{0.5}\sigma_5(1-\sigma_6^2)(\sigma_4+\sigma_7)$$

$$B_6 = a^2(M_2N_3l_1(\sigma_5-\sigma_3)(\sigma_7-\sigma_4)(1+\sigma_6^2) + N_3\sqrt{M_2N_2}(\sigma_5-\sigma_3)(\sigma_7+\sigma_4)(1-\sigma_6^2) + N_2\sqrt{M_3N_3}(\sigma_5+\sigma_3)(\sigma_7-\sigma_4)(1-\sigma_6^2) + \frac{1}{M_1}(\sigma_5+\sigma_3)(\sigma_7+\sigma_4)(1+\sigma_6^2)$$

$$\sigma_1 = e^{\alpha r\sqrt{M_2N_2}}, \sigma_2 = e^{\alpha\theta\sqrt{M_2N_2}}, \sigma_3 = e^{\alpha\sqrt{M_3N_3}}, \sigma_4 = e^{2\alpha\theta\sqrt{M_2N_2}}, \sigma_5 = e^{2\alpha\theta\sqrt{M_3N_3}}, \sigma_6 = e^{\alpha r\sqrt{M_1N_1}}, \sigma_7 = e^{2\alpha r\sqrt{M_2N_2}}, \sigma_8 = e^{\theta\sqrt{M_3N_3}}, \sigma_9 = e^{2\alpha\sqrt{M_3N_3}}, \sigma_{10} = e^{\alpha\theta\sqrt{M_3N_3}}, \sigma_{11} = \alpha r\sqrt{M_1N_1}$$

Appendix B

$$\int_0^r g_1^{(1)}(\eta_1)\cdot\psi'_{\phi_1}d\eta_1 = -\frac{F_1}{6M_1N_1^2\alpha^5\phi_1^2\sqrt{M_1N_1}}$$

$$\int_r^\theta g_2^{(1)}(\eta_2)\cdot\psi'_{\phi_2}d\eta_2 = \frac{F_2}{6M_2N_2^2N_3\alpha^5\phi_2^2\sqrt{M_2N_2}} + \frac{F_3}{6M_2N_2^2N_3\alpha^5\phi_2^2} - \frac{F_4}{6M_2N_2^2N_3\alpha^5\phi_2^2\phi_3\sqrt{M_2N_2}} - \frac{F_5}{6M_2N_2^2N_3\alpha^5\phi_2^2\phi_3\sqrt{M_3N_3}} - \frac{F_6}{6M_2N_2^2N_3\alpha^5\phi_2^2\phi_3\sqrt{M_2N_2}\sqrt{M_3N_3}}$$
$$-\frac{F_7}{6M_2N_2^2N_3\alpha^5\phi_2^2\phi_3}$$

$$\int_\theta^1 g_3^{(1)}(\eta_3)\cdot\psi'_{\phi_3}d\eta_3 = \frac{F_8}{6M_3N_3^2\alpha^5\phi_3^2\sqrt{M_3N_3}} + \frac{F_9}{6M_3N_3^2\alpha^5\phi_3^2}$$

$$F_1 = 12\Omega_1 - 12\Omega_2 - 12\Omega_1\sigma_6 + 12\Omega_2\sigma_6^{-1} + 3N_1\alpha^2(\Omega_1^2\sigma_{12} - 4\Omega_1^2\sigma_6 + 3\Omega_1^2 - 3\Omega_2^2 + 4\Omega_1\Omega_2\sigma_6 - 4(\Omega_1-\Omega_2)\overline{\psi_\phi}\phi_1 + 4\Omega_1\overline{\psi_\phi}\phi_1\sigma_6) + 3N_1\alpha^2\Omega_2^2(4\sigma_6^{-1}-\sigma_{12}^{-1})$$
$$+ 2M_1r^2\sigma_{11} - 6\sigma_{11}^2(\Omega_1-\Omega_2) - 4\alpha^3r^3\overline{\psi_\phi}\phi_1\sigma_{13} - 12N_1\alpha^2\Omega_1\Omega_2\sigma_6^{-1} - 6N_1\alpha^2\sigma_{11}(-\Omega_1^2 + 4\Omega_1\Omega_2 + 2\Omega_1\overline{\psi_\phi}\phi_1\sigma_6 - \Omega_2^2) + 12\Omega_1\sigma_{11}\sigma_6 + 12\Omega_2\sigma_6^{-1}\sigma_{11} + 2N_1\alpha^5\overline{\psi_\phi^2}\phi_1^2r^3\sigma_{13}$$
$$-12N_1\alpha^2\Omega_2\overline{\psi_\phi}\phi_1\sigma_6^{-1}(1+\sigma_{11}) + 6\alpha^2N_1\overline{\psi_\phi}\phi_1\sigma_{11}^2(\Omega_1-\Omega_2)$$

$$F_2 = 12N_3\Omega_3(\sigma_2-\sigma_1) - 12N_3\Omega_4(\sigma_2^{-1}-\sigma_1^{-1}) + 3N_2N_3\alpha^2\Omega_4^2(4(\sigma_1\sigma_2)^{-1} - 3\sigma_4^{-1} - \sigma_7^{-1}) - 3N_2N_3\alpha^2\Omega_3(4C_3\sigma_1\sigma_2 - 3\Omega_3\sigma_4 - \Omega_3\sigma_7 + 4\Omega_4\sigma_2\sigma_1^{-1} + 4\overline{\psi_\phi}\phi_2(\sigma_2-\sigma_1))$$
$$+ 12N_2N_3\alpha^2\Omega_4(\Omega_3\sigma_1\sigma_2^{-1} + \overline{\psi_\phi}\phi_2(\sigma_2^{-1}-\sigma_1^{-1}) + 6M_2N_2N_3\alpha^2\Omega_4\sigma_2^{-1}(\theta^2+r^2) + N_3\alpha^3\overline{\psi_\phi}\phi_2(\theta-r)^2\sigma_{16}((\theta-4r+3) + \alpha^2N_2\overline{\psi_\phi}(\theta+2r-3))$$
$$-6M_2N_2N_3\alpha^2(\Omega_3\sigma_2(\theta-r)^2 + 2\Omega_4\theta r\sigma_2^{-1}) - 6M_2N_2^2N_3\alpha^4\Omega_4\overline{\psi_\phi}\phi_2\sigma_2^{-1}(\theta-r+r^2-r\theta) - 6M_2N_2^2N_3\alpha^4\Omega_3\overline{\psi_\phi}\phi_2\sigma_2(\theta-r)(r-1)$$

$$F_3 = -2M_2N_3\alpha(\theta-r)^3 - 12N_3\alpha(\theta-r)(\Omega_4\sigma_1^{-1}+\Omega_3\sigma_1) + 6N_2N_3\alpha^3\Omega_3((4\Omega_4-\Omega_3\sigma_4)(\theta-r) - \overline{\psi_\phi}\phi_2(\sigma_2-\sigma_1) + \overline{\psi_\phi}\theta\phi_2(\sigma_2+\sigma_1) - 2\overline{\psi_\phi}\phi_2r\sigma_1) - 6N_2N_3\alpha^3\Omega_4^2\sigma_4^{-1}(\theta-r)$$
$$-6N_2N_3\alpha^3\Omega_4\overline{\psi_\phi}\phi_2(\sigma_2^{-1}-\sigma_1^{-1}+\theta(\sigma_2^{-1}+\sigma_1^{-1}) + 2r\sigma_1^{-1})$$

$$F_4 = -3\alpha\phi_2(\theta-r)^2(\theta-1)\sigma_{16} + 6M_2N_2^2\alpha^2\Omega_4\theta^2\phi_2\sigma_2^{-1} + 3N_2\overline{\psi_\phi}\alpha^3\phi_2^2(\theta-r)^2(\theta-1)\sigma_{16} - 6M_2N_2^2\alpha^2\Omega_4\phi_2\sigma_2^{-1}(\theta-r+\theta r) - 6M_2N_2^2\alpha^2\Omega_3\phi_2\sigma_2(\theta-r)(\theta-1)$$

$$F_5 = -N_2N_36\alpha^2\phi_2(\Omega_3\Omega_5(\sigma_8\sigma_{14}+\sigma_2\sigma_3-\sigma_1\sigma_3-\sigma_2\sigma_{10}) + \Omega_4\Omega_5(\sigma_8\sigma_{14}^{-1}+\sigma_3\sigma_2^{-1}-\sigma_3\sigma_1^{-1}+\sigma_{10}\sigma_2^{-1}) + \Omega_3\Omega_6((\sigma_2+\sigma_1)\sigma_{10}^{-1} + +(\sigma_2-\sigma_1)\sigma_3^{-1})$$
$$+\Omega_4\Omega_6((\sigma_8\sigma_{14})^{-1} + (\sigma_2\sigma_3)^{-1} - (\sigma_1\sigma_3)^{-1} - (\sigma_2\sigma_{10})^{-1})$$

$$F_6 = 3N_3\alpha^2\Omega_6\phi_2(r^2+\theta^2)\sigma_{10}^{-1}\sigma_{16} + 6M_2N_2^2N_3\alpha^3\phi_2(\theta-r)(\Omega_3\Omega_5\sigma_2\sigma_3 + \Omega_3\Omega_6\sigma_2\sigma_{10}^{-1} - \Omega_4\Omega_5\sigma_3\sigma_2^{-1} - \Omega_3\Omega_5\sigma_2\sigma_{10}) + 3N_3\alpha^2\Omega_5\phi_2(\sigma_3-\sigma_{10})(\theta-r)^2\sigma_{16}$$
$$-3N_3\alpha^2\Omega_6\phi_2\sigma_{16}\sigma_3^{-1}(r^2+\theta^2) - 6N_3\alpha^2\Omega_6\theta\phi_2r\sigma_{16}(\sigma_{10}^{-1}-\sigma_3^{-1}) + 6M_2N_2^2N_3\alpha^3\phi_2(\theta-r)(\Omega_4\Omega_5\sigma_{10}\sigma_2^{-1} + \Omega_4\Omega_6(\sigma_2\sigma_3)^{-1}) - 3N_2N_3\alpha^4\Omega_6\overline{\psi_\phi}\phi_2^2\sigma_{10}^{-1}\sigma_{16}(\theta^2+r^2)$$
$$-6M_2N_2^2N_3\alpha^3\phi_2(\theta-r)(\Omega_3\Omega_6\sigma_2\sigma_3^{-1} + \Omega_4\Omega_6(\sigma_2\sigma_{10})^{-1}) - 3N_2N_3\alpha^4\overline{\psi_\phi}\phi_2^2\sigma_{16}(\Omega_5(\sigma_3-\sigma_{10})(\theta-r)^2 - \Omega_6\theta^2\sigma_3^{-1}) - 6N_2N_3\alpha^4\Omega_6\overline{\psi_\phi}\theta\phi_2^2r\sigma_{16}(\sigma_3^{-1}-\sigma_{10}^{-1})$$

$$F_7 = -6N_2\alpha\Omega_4\phi_2(\sigma_2^{-1}-\sigma_1^{-1}) + 6N_2\alpha\Omega_3\phi_2(\sigma_2-\sigma_1)(\theta-1) + 6N_2\alpha\Omega_4\theta\phi_2(\sigma_2^{-1}-\sigma_1^{-1})$$

$$
\begin{aligned}
F_8 = {} & 12(\Omega_5(\sigma_3-\sigma_{10}) + \Omega_6(\sigma_{10}^{-1}-\sigma_3^{-1}))-N_3\alpha^2(\Omega_5^2(6\sigma_{10}\sigma_3 + 6\sigma_{17}\sigma_3-9\sigma_9-6\sigma_{10}\sigma_{17} + 3\sigma_5) + \Omega_5\Omega_6(-6\sigma_{10}\sigma_{17}^{-1} + 6\sigma_3\sigma_{10}^{-1} + 6\sigma_3\sigma_{17}^{-1})-12\Omega_5\overline{\psi_\phi}\phi_3(\sigma_{10}-\sigma_3)) \\
& + 3N_3\alpha^2\Omega_6^2(\sigma_5^{-1} + 2(\sigma_{10}\sigma_3)^{-1} + 2(\sigma_{17}\sigma_3)^{-1}-3\sigma_9^{-1}-2(\sigma_{10}\sigma_{17})^{-1}) + 6N_3\alpha^2\Omega_5\Omega_6((\sigma_{17} + \sigma_{10})\sigma_3^{-1}-\sigma_{17}\sigma_{10}^{-1})-3M_3N_3\alpha^2\Omega_5\sigma_1\sigma_2 \\
& -3M_3N_3\alpha^2\Omega_6(\sigma_3(2-4r-\theta^2 + r^2 + 2\theta r) + \sigma_{10}(\theta^2-r^2-2\theta + 2r)) + 6M_3N_3\alpha^2\Omega_6\sigma_3^{-1}(1-2r) + 12N_3\alpha^2\Omega_6\overline{\psi_\phi}\phi_3\sigma_3^{-1}-3M_3N_3\alpha^2\Omega_6\sigma_3^{-1}(\theta^2-r^2) \\
& -2\alpha^3\overline{\psi_\phi}\phi_3(\theta-1)\sigma_{18}(-\theta^2 + 2\theta + 3r^2-6r + 2) + 3M_3N_3\alpha^2\sigma_{10}^{-1}\Omega_6(-2\theta + 2\overline{\psi_\phi}\phi_3 + \theta^2-r^2)-12N_3\alpha^2\Omega_6\overline{\psi_\phi}\phi_3\sigma_{10}^{-1} \\
& + N_3\alpha^5\overline{\psi_\phi}^2\phi_3^2(\theta-1)\sigma_{18}(-\theta^2 + 2\theta + 3r^2-6r + 2) + 3M_3N_3^2\alpha^4\Omega_5\overline{\psi_\phi}\phi_3(\sigma_3(2-4r-\theta^2 + r^2 + 2\theta r) + \sigma_{10}(\theta^2-r^2-2\theta + 2r)) \\
& -3M_3N_3^2\alpha^4\Omega_6\overline{\psi_\phi}\phi_3\sigma_3^{-1}(2-4r-\theta^2 + r^2 + 2\theta r)-3M_3N_3^2\alpha^4\Omega_6\overline{\psi_\phi}\phi_3\sigma_{10}^{-1}(\theta^2-r^2 + 2\theta-2r)
\end{aligned}
$$

$$
\begin{aligned}
F_9 = {} & -6\alpha\Omega_6(\sigma_{10}^{-1} + \sigma_{17}^{-1})-6N_3\alpha^3\Omega_6^2\sigma_9^{-1}-6N_3\alpha^3\Omega_5(\Omega_6(2\theta-4 + 2r + (\theta-r)\sigma_3\sigma_{10}^{-1}) + \Omega_5(\sigma_9(1-r)-(\theta-r)\sigma_{10}\sigma_3)-\overline{\psi_\phi}\phi_3(\sigma_{10} + \sigma_{17})(1 + \theta) \\
& + 6\alpha\Omega_5(\sigma_{10} + \sigma_{17})(\theta-1) + M_3\alpha(\theta-1)(-\theta^2 + 2\theta + 3r^2-6r + 2) + 6\alpha\Omega_6\theta(\sigma_{10}^{-1} + \sigma_{17}^{-1}) + 6N_3\alpha^3\Omega_6^2\theta(\sigma_{10}\sigma_3)^{-1}(\theta-r) \\
& + 6N_3\Omega_6\alpha^3(\Omega_6 r\sigma_9^{-1}-\Omega_5\sigma_{10}\sigma_3^{-1}(\theta-r)) + 6N_3\alpha^3\Omega_6\overline{\psi_\phi}\phi_3(\sigma_{10}^{-1} + \sigma_{17}^{-1})(1-\theta)
\end{aligned}
$$

$$
\sigma_{12} = e^{2\alpha r\sqrt{M_1N_1}},\sigma_{13} = (M_1N_1)^{1.5},\sigma_{14} = e^{r\sqrt{M_2N_2}},\sigma_{15} = e^{\theta\sqrt{M_2N_2}},\sigma_{16} = (M_2N_2)^{1.5},\sigma_{17} = e^{\alpha r\sqrt{M_3N_3}},\sigma_{18} = (M_3N_3)^{1.5}
$$

References

Aris, R., 1956. On the dispersion of a solute in a fluid flowing through a tube. Proc. Royal Soc. Lond. Ser. A – Math. Phys. Sci. 235, 67–77.

Carvalho, F.P., Villeneuve, J.P., Cattini, C., Rendón, J., De Oliveira, J.M., 2009. Ecological risk assessment of PCBs and other organic contaminant residues in laguna de terminos, mexico. Ecotoxicology 18, 403–416.

Chatwin, P.C., 1970. Approach to normality of concentration distribution of a solute in a solvent flowing along a straight pipe. J. Fluid Mech. 43, 321–352.

Chen, B., 2013. Contaminant transport in a two-zone wetland: dispersion and ecological degradation. J. Hydrol. 488, 118–125.

Chen, G.Q., Wu, Z., 2012. Taylor dispersion in a two-zone packed tube. Int. J. Heat Mass Transf. 55, 43–52.

Chen, G.Q., Wu, Z., Zeng, L., 2012. Environmental dispersion in a two-layer wetland: analytical solution by method of concentration moments. Int. J. Eng. Sci. 51, 272–291.

Chen, G.Q., Zeng, L., Wu, Z., 2010. An ecological risk assessment model for a pulsed contaminant emission into a wetland channel flow. Ecol. Model. 221, 2927–2937.

Costanza, R., D'Arge, R., de Groot, R., Stephen, F., Grasso, M., Hannon, B., Limburg, K., Naeem, S., O'Neill, R., Paruelo, J., Raskin, R., Sutton, P., Van Den Belt, M., 1997. The value of the world's ecosystem services and natural capital. Nature 387, 253–260.

Costanza, R., Farber, S.C., Maxwell, J., 1989. Valuation and management of wetland ecosystems. Ecol. Econ. 1, 335–361.

Ergun, S., 1952. Fluid flow through packed columns. Chem. Eng. Prog. 48, 89–94.

Fischer, H.B., List, E.J., Koh, R.C.Y., Imberger, J., Brooks, N.H., 1979. Mixing in inland and coastal waters. Acad. San Diego Calif. 114, 315–316.

Gill, W.N., 1967. A note on solution of transient dispersion problems. Proc. Royal Soc. Lond. Ser. A – Math. Phys. Sci. 298 (1454), 335–339.

Kao, C.M., Wu, M.J., 2001. Control of non-point source pollution by a natural wetland. Water Sci. Technol. 43 (5), 169–174.

Lavrnic, S., Mancini, M.L., 2016. Can constructed wetlands treat wastewater for reuse in agriculture? Review of guidelines and examples in South Europe. Water Sci. Technol. 73 (11), 2616–2626.

Lightbody, A.F., Nepf, H.M., 2006. Prediction of near-field shear dispersion in an emergent canopy with heterogeneous morphology. Environ. Fluid Mech. 6, 477–488.

Liu, S., Masliyah, J.H., 2005. Dispersion in porous media. In: Vafai, K. (Ed.), Handbook of Porous Media. CRC Press, USA, pp. 81–140.

Luo, J., Huai, W., Wang, P., 2016. Contaminant transport in a three-zone wetland: dispersion and ecological degradation. J. Hydrol. 534, 341–351.

Mei, C.C., Auriault, J.L., Ng, C.O., 1996. Some applications of the homogenization theory. Adv. Appl. Mech. 32, 277–348.

Mitsch, W.J., Gosselink, J.G., 1993. Wetlands. Van Nostrand Reinhold, New York, USA.

Mitsch, W.J., Hernandez, M.E., 2013. Landscape and climate change threats to wetlands of North and Central America. Aquat. Sci. 75 (1), 133–149.

Murphy, E., Ghisalberti, M., Nepf, H., 2007. Model and laboratory study of dispersion in flows with submerged vegetation. Water Resour. Res. 43. http://dx.doi.org/10.1029/2006WR005229.

Nepf, H., Ghisalberti, M., 2008. Flow and transport in channels with submerged vegetation. Acta Geophys. 56, 753–777.

Sheng, Y.P., Lick, W., 1979. The transport and resuspension of sediments in a shallow lake. J. Geophys. Res. [Oceans] 84 (C4), 1809–1826.

Stone, B.M., Shen, H.T., 2002. Hydraulic resistance of flow in channels with cylindrical roughness. J. Hydraul. Eng. 128, 500–506.

Taylor, G., 1953. Dispersion of soluble matter in solvent flowing slowly through a tube. Proc. Royal Soc. Lond. Ser. A – Math. Phys. Eng. Sci. 219, 186–203.

US Environmental Protection Agency (EPA), 1999. Manual: Constructed Wetlands Treatment of Municipal Wastewaters. EPA/625/R-99/010, EPA Office of Research and Development, Cincinnati, OH, USA.

Wang, P., Chen, G.Q., 2016. Solute dispersion in open channel flow with bed absorption. J. Hydrol. 543, 208–217.

Wang, P., Chen, G.Q., Jiang, C.B., Alsaedi, A., Wu, Z., Zeng, L., 2015. Transport in a three-zone wetland: flow velocity profile and environmental dispersion. Commun. Nonlinear Sci. Numer. Simul. 20, 136–153.

Wang, P., Wu, Z., Chen, G.Q., Cui, B.S., 2013. Environmental dispersion in a three-layer wetland flow with free-surface. Commun. Nonlinear Sci. Numer. Simul. 18, 3382–3406.

Wu, J., 1969. An estimation of wind effects on dispersion in wide channels. Water Resour. Res. 5 (5), 1097–1104.

Wu, Z., Chen, G.Q., 2012. Dispersion in a two-zone packed tube: an extended Taylor's analysis. Int. J. Eng. Sci. 50, 113–123.

Wu, Z., Chen, G.Q., 2014a. Analytical solution for scalar transport in open channel flow: slow-decaying transient effect. J. Hydrol. 519, 1974–1984.

Wu, Z., Chen, G.Q., 2014b. Approach to transverse uniformity of concentration distribution of a solute in a solvent flowing along a straight pipe. J. Fluid Mech. 740, 196–213.

Wu, Z., Chen, G.Q., Zeng, L., 2011a. Environmental dispersion in a two-zone wetland. Ecol. Model. 222, 456–474.

Wu, Z., Fu, X., Wang, G.Q., 2015. Concentration distribution of contaminant transport in wetland flows. J. Hydrol. 525, 335–344.

Wu, Z., Fu, X.D., Wang, G.Q., 2016. On spatial pattern of concentration distribution for Taylor dispersion process. Sci. Rep. 6, 20556.

Wu, Z., Li, Z., Chen, G.Q., 2011b. Multi-scale analysis for environmental dispersion in wetland flow. Commun. Nonlinear Sci. Numer. Simul. 16, 3168–3178.

Zeng, L., Chen, G.Q., 2009. Notes on modelling of environmental transport in wetland. Commun. Nonlinear Sci. Numer. Simul. 14, 1334–1345.

Zeng, L., Chen, G.Q., 2011. Ecological degradation and hydraulic dispersion of contaminant in wetland. Ecol. Model. 222, 293–300.

Zeng, L., Chen, G.Q., Tang, H.S., Wu, Z., 2011. Environmental dispersion in wetland flow. Commun. Nonlinear Sci. Numer. Simul. 16, 206–215.

Zeng, L., Wu, Z., Fu, X., Wang, G., 2015. Performance of the analytical solutions for Taylor dispersion process in open channel flow. J. Hydrol. 528, 301–311.

Zeng, L., Wu, Y.H., Ji, P., Chen, B., Zhao, Y.J., Chen, G.Q., Wu, Z., 2012. Effect of wind on contaminant dispersion in a wetland flow dominated by free-surface effect. Ecol. Model. 237–238, 101–108.